Exploiting coastal altimetry to improve the surface circulation scheme over the central Mediterranean Sea

Fatma Jebri, Florence Birol, Bruno Zakardjian, Jérome Bouffard, Cherif Sammari

AGU PUBLICATIONS

JGR

Journal of Geophysical Research: Oceans

RESEARCH ARTICLE

10.1002/2016JC011961

Exploiting coastal altimetry to improve the surface circulation scheme over the central Mediterranean Sea

Fatma Jebri[1,2,3,4], Florence Birol[3], Bruno Zakardjian[4], Jérome Bouffard[5], and Cherif Sammari[1]

[1]Institut National des Sciences et Technologies de la Mer Salammbô, Tunisia, [2]Ecole Nationale d'Ingénieurs de Tunis, Université de Tunis El Manar, Tunis, Tunisia, [3]Laboratoire d'Etudes en Géophysique et Océanographie Spatiales, OMP, Toulouse, France, [4]Université de Toulon, CNRS/INSU, Aix Marseille Université, IRD, Mediterranean Institute of Oceanography La Garde, France, [5]RHEA for European Space Agency, Earth Observation Directorate, ESRIN/EOP GMQ, Frascati, Italy

Abstract This work is the first study exploiting along track altimetry data to observe and monitor coastal ocean features over the transition area between the western and eastern Mediterranean Basins. The relative performances of both the AVISO and the X-TRACK research regional altimetric data sets are compared using in situ observations. Both products are cross validated with tide gauge records. The altimeter-derived geostrophic velocities are also compared with observations from a moored Acoustic Doppler Current Profiler. Results indicate the good potential of satellite altimetry to retrieve dynamic features over the area. However, X-TRACK shows a more homogenous data coverage than AVISO, with longer time series in the 50 km coastal band. The seasonal evolution of the surface circulation is therefore analyzed by conjointly using X-TRACK data and remotely sensed sea surface temperature observations. This combined data set clearly depicts different current regimes and bifurcations, which allows us to propose a new seasonal circulation scheme for the central Mediterranean. The analysis shows variations of the path and temporal behavior of the main circulation features: the Atlantic Tunisian Current, the Atlantic Ionian Stream, the Atlantic Libyan Current, and the Sidra Gyre. The resulting bifurcating veins of these currents are also discussed, and a new current branch is observed for the first time.

Key Points:
- Assessment of conventional altimetry over the wide shelf of Tunisia
- Monitoring seasonal variability of the Atlantic Tunisian Current/Atlantic Ionian Stream and associated features from altimetry
- Coastal altimetry is able to detect the slope circulation in the central Mediterranean Sea

Correspondence to:
F. Jebri,
fatma.jebri@legos.obs-mip.fr

Citation:
Jebri, F., F. Birol, B. Zakardjian, J. Bouffard, and C. Sammari (2016), Exploiting coastal altimetry to improve the surface circulation scheme over the central Mediterranean Sea, *J. Geophys. Res. Oceans*, *121*, 4888–4909, doi:10.1002/2016JC011961.

Received 11 MAY 2016
Accepted 10 JUN 2016
Accepted article online 14 JUN 2016
Published online 16 JUL 2016

1. Introduction

The circulation of the Mediterranean Sea is relatively complex because of the basin geometry, which is divided into several small subbasins, and its rugged topography (Figure 1). Inflowing Atlantic Water flows at the surface through the Strait of Gibraltar. It is transformed along its path in the basin into denser Mediterranean water that in turns enters the North Atlantic through Gibraltar. Surface currents, strongly influenced by atmospheric forcing, have temporal variability from diurnal to inter-annual scales and follow tortuous paths constrained by the bathymetry [*Millot*, 1999]. Further east of Gibraltar, the Atlantic Water flow forms the coastal "Algerian current," which widens and deepens eastward [*Millot*, 1999]. Part of the Algerian Current continues to flow along the northern coast of Sicily as the Bifurcation Tyrrhenian Current [*Béranger et al.*, 2004; *Sorgente et al.*, 2011]. Downstream of the Algerian Basin, the Tunisia-Sicily Channel and its immediate surroundings are key dynamic regions that modulate the passage of the surface and intermediate water masses between the Eastern and Western Mediterranean Sea [*Sorgente et al.*, 2011]. There, surface circulation shows two main branches. The first branch consists of an Atlantic Water jet (known as AIS, the Atlantic Ionian Stream, Figure 1) that flows along the southern coast of Sicily [*Robinson et al.*, 1999] and meanders around mesoscale vortices such as the Adventure Bank Vortex and the Ionian Shelf Vortex [*Lermusiaux and Robinson*, 2001]. The AIS transports the Atlantic Water into the eastern Mediterranean Sea through the Strait of Sicily. This current flows toward the southeast or can turn northward in an anticyclonic loop when it enters the Ionian Sea [*Lermusiaux and Robinson*, 2001]. The second branch of Atlantic Water is a slope current flowing close to the 200 m isobath until it reaches Lampedusa Island; this current is known as the Atlantic Tunisian Current (ATC, Figure 1) [*Sammari et al.*, 1999] and is still poorly documented except by sparse in situ observations. South of Lampedusa, the ATC also splits into two branches: the first one enters onto the continental shelf in the Gulf of Gabes and the second one directly reaches the African coast and heads east toward Libya [*Alhammoud et al.*, 2004; *Béranger et al.*, 2004; *Hamad et al.*, 2006]. Part of this

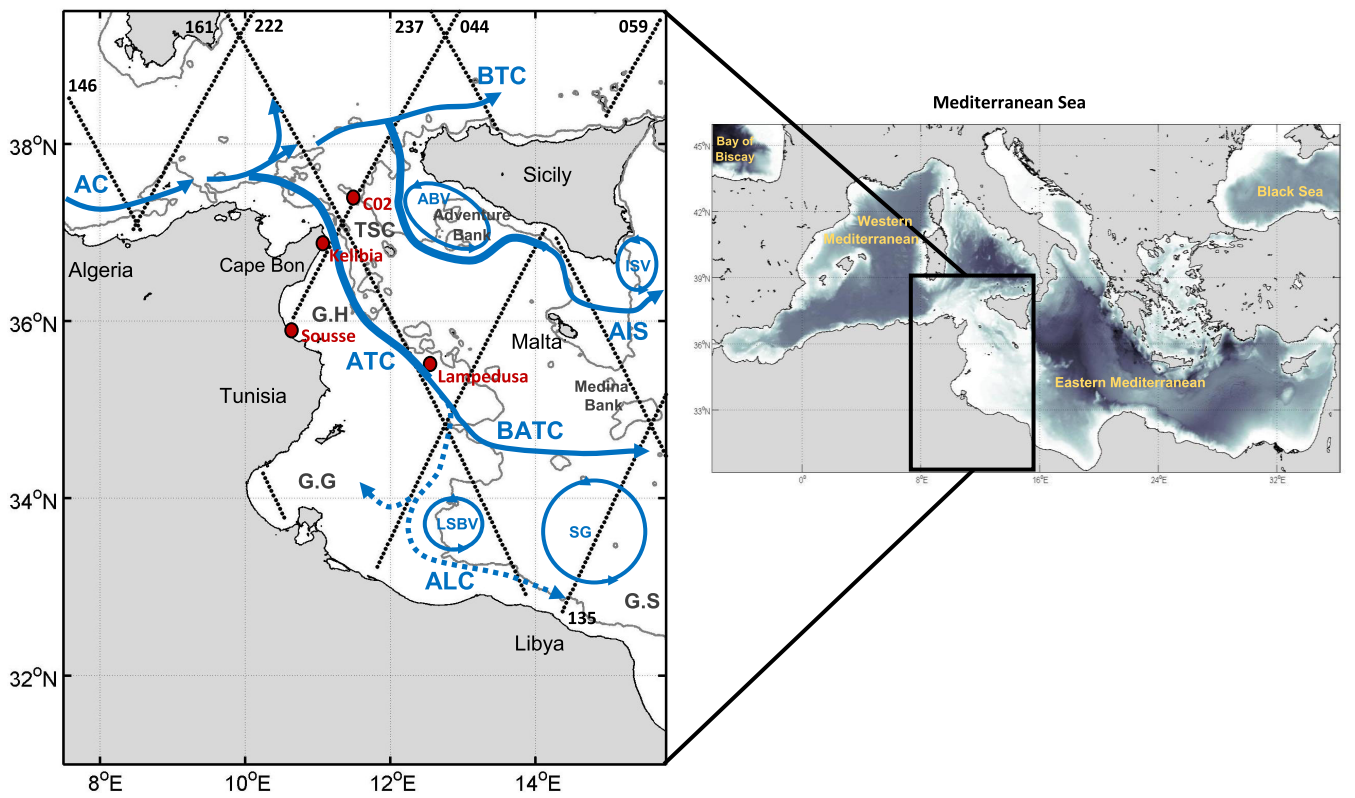

Figure 1. Schematic view of the major ocean circulation features in the central Mediterranean based on *Lermusiaux and Robinson* [2001] and *Sorgente et al.* [2011] and distribution of selected tracks over the study area: 044, 059, 135, 146, 161, 222, and 237 from T/P+J1+J2 mission. From West to East—AC: Algerian Current, ATC: Atlantic Tunisian Current, BATC: Bifurcation Atlantic Tunisian Current, ALC: Atlantic Libyan Current, LSBV: Libyan Shelf Break Vortex, SG: Sidra Gyre, BTC: Bifurcation Tyrrhenian Current, AIS: Atlantic Ionian Stream, ABV: Adventure Bank Vortex, and ISV: Ionian Shelf Break Vortex. Locations of available tide gauge and C02 Current meter stations are indicated by red dots. The different subregions are the TSC: Tunisian-Sicily Channel, G.H: Gulf of Hammamet, G.G: Gulf of Gabes, and G.S: Gulf of Sirte. The 200 m isobath (grey solid line) is from ETOPO2v1 global gridded database.

eastward ATC flows into the Ionian Sea as the Bifurcation Atlantic Tunisian Current supported by the anticyclonic Sidra Gyre [*Ciappa*, 2009; *Sorgente et al.*, 2011]. A second part of the ATC extension called the Atlantic Libyan Current [*Gasparini et al.*, 2008; *Poulain and Zambianchi*, 2007] is bounded by the cyclonic Libyan Shelf Break Vortex [*Sorgente et al.*, 2011]. Because of its position that separates shelf waters from offshore waters, the ATC is expected to play a key role in cross-shelf exchanges of natural and anthropogenic elements. It is therefore of critical importance to monitor the variability associated with this hydrodynamic feature in an almost synoptic way.

The detection of the ATC and AIS signatures is particularly challenging due to their high space-time variability and the lack of regular in situ observations. These circulation features have only been partially observed using remotely sensed data (temperature satellite images [e.g., *Taupier-Letage*, 2008] and chlorophyll data [e.g., *Ciappa*, 2009]) and in situ observations, mainly drifting buoys [*Poulain and Zambianchi*, 2007] and Acoustic Doppler Current Profilers, in synergy with numerical modeling [e.g., *Ben Ismail et al.*, 2012; *Molcard et al.*, 2002]. Satellite altimetry now provides more than two decades of synoptic measurements of sea level variations and has allowed major advances in the knowledge of the general circulation of the oceans [e.g., *Fu and Smith*, 1996; *Fu and Morrow*, 2013]. However, the use of conventional pulse-limited altimetry to monitor narrow density coastal currents is a nontrivial exercise [*Vignudelli et al.*, 2005], mainly because of the instrumental limitations and the difficulty of isolating a current signature from noise and other ocean signals. Therefore, exploiting altimetry over the Tunisian/Libyan shelf, a shallow water area marked by a strong mesoscale activity, would require applying coastal-oriented approaches that have already proven their effectiveness and robustness in providing a synoptic view of current position and intensity over the northwestern Mediterranean Sea [see *Bouffard et al.*, 2008, 2011; *Birol et al.*, 2010; *Vignudelli et al.*, 2005].

Our main objective of this study is to analyze the surface circulation and provide a synoptic view of its seasonal variability along and over the poorly documented central Mediterranean area. In this article,

the AVISO and the X-TRACK [*Roblou et al*., 2011] regional altimetric data sets are analyzed in parallel to assess the impact of the data processing approach in the monitoring of the geostrophic circulation associated with the ATC/AIS systems. In section 2, data and methods of analysis are described. In section 3, altimetry sea level anomalies are validated against those provided by tide gauge records. In addition, across-track geostrophic velocities computed from along-track absolute dynamic topography are compared with data from a moored Acoustic Doppler Current Profiler (ADCP) and with the information provided by satellite surface temperature images. Analysis of the seasonal variations of the surface circulation scheme is made in section 4. Finally, a summary and some perspectives are given in section 5.

2. Materials and Methods

2.1. Altimetry Data

We used 20 years (1993–2013) of observations from the Topex/Poseidon, Jason-1, and Jason-2 altimetry missions (the entire time series is hereafter called T/P+J1+J2) along seven satellite tracks crossing the central Mediterranean Sea (044, 059, 135, 161, 146, 222, and 237; see Figure 1). Two along-track regional sea level products were considered. The first product is the delayed time "Update" product distributed by the AVISO (Archiving, Validation and Interpretation of Satellite Oceanographic Data) operational service; it consists of sea level anomalies (SLA) and the Absolute Dynamic Topography (ADT), which is the sum of SLA and the Mean Dynamic Topography (MDT). For this study, we used the regional ADT product available for the Mediterranean Sea, which includes a specific regional MDT [*Rio et al*., 2014]. Dedicated algorithms and corrections have been used to improve the quality of altimetry data over the Mediterranean Sea [*Dufau et al*., 2013].

The second altimetry product is a regional experimental SLA product (X-TRACK) computed by the CTOH (Centre de Topographie des Océans et de l'Hydrosphère) and also distributed by AVISO (http://www.aviso.altimetry.fr/en/data/products/sea-surface-height-products/regional/x-track-sla.html). The data are generated with a specific regional reprocessing algorithm and tuned to improve the quality and availability of coastal altimetry data [for example, *Durand et al*., 2008; *Birol et al*., 2010; *Bouffard et al*., 2011]; method details can be found in *Roblou et al*. [2011] or on the AVISO+ website. The X-TRACK data set used here includes shorter spatial scale variations (along track loss filter with a 40 km wavelength cut off) than AVISO (70 km wavelength cut off) and a high-resolution tidal correction derived from a regional version of the MOG2D model rather than the global FES2012 model used in the AVISO processing. Unlike AVISO, it does not include a long wavelength error correction used to remove correlated noise due to orbit errors or uncertainties in geophysical corrections. Note that we have computed the X-TRACK ADT by adding the regional MDT [*Rio et al*., 2014] to the X-TRACK SLA for the purpose of homogeneity.

First, we compared the quantity of valid altimetry SLA (i.e., not flagged) provided by the two products (AVISO and X-TRACK) along the Tunisian shelf. Figure 2 shows that the percentage of valid data (relative to the total number of cycles considered) over the 20 year period was significantly higher in X-TRACK than in AVISO. The differences between the two products were observed not only near the coasts but also offshore (Figure 2a). Figure 2b shows that the AVISO data availability varied from 82% (at 28 km) to 95% for functions of the distance to the coast. For X-TRACK, the data availability is 92% more than 35 km from the coastline and remains almost constant. Note that the measurements made by the Poseidon altimeter are not processed in X-TRACK; this leads to 30 missed cycles, which explains the lower percentage over the deep ocean and more than 220 km from land (the red curve on Figure 2b). Despite the missed cycles, the availability of X-TRACK data clearly appears more homogeneous both in space and time, and there are more data in the 100 km coastal band where most of the dynamic structures are located. The standard deviations of the corresponding SLA time series have also been computed (Figure 3). The patterns of variability observed are very similar for both products; however, larger values are obtained from X-TRACK (8.54 cm on average) than from AVISO (7.70 cm). Note that the larger differences observed at X-TRACK crossovers than from AVISO are due to the application of global crossover adjustment methods [*Le Traon and Ogor*, 1998]. In addition to residual orbit errors, these differences might also be explained by more high-frequency coastal small-scale processes captured by X-TRACK. This point will be specifically discussed in sections 3 and 4.

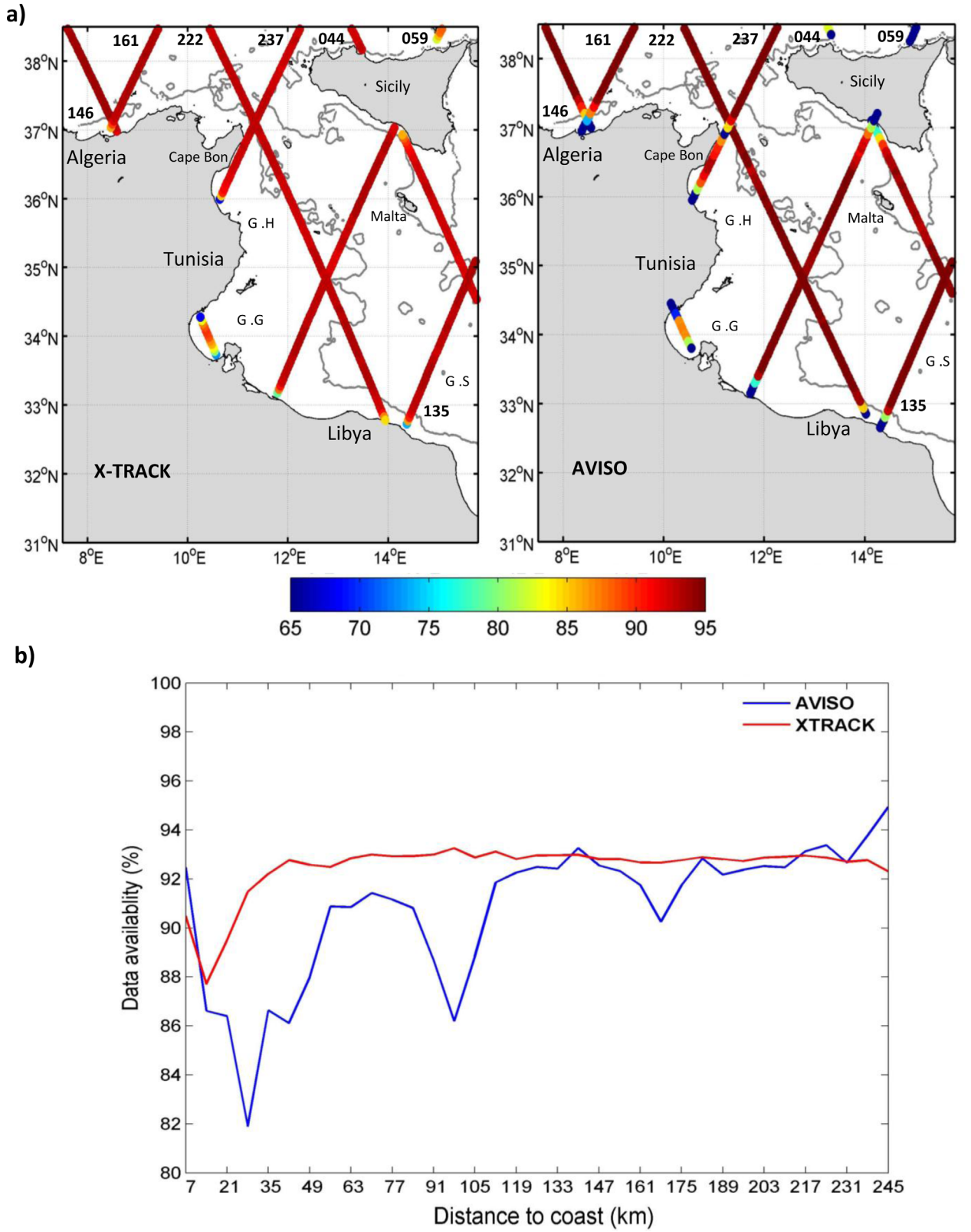

Figure 2. Percentage of altimetry data availability from T/P+J1+J2 mission for the period 1993–2013. (a) X-TRACK and AVISO percentage maps; more cycles are available in AVISO. G.H is the Gulf of Hammamet, G.G is the Gulf of Gabes, and G.S is the Gulf of Sirte. (b) Average percentage of X-TRACK (red line) and AVISO (blue line) data availability as a function of the distance to the coast.

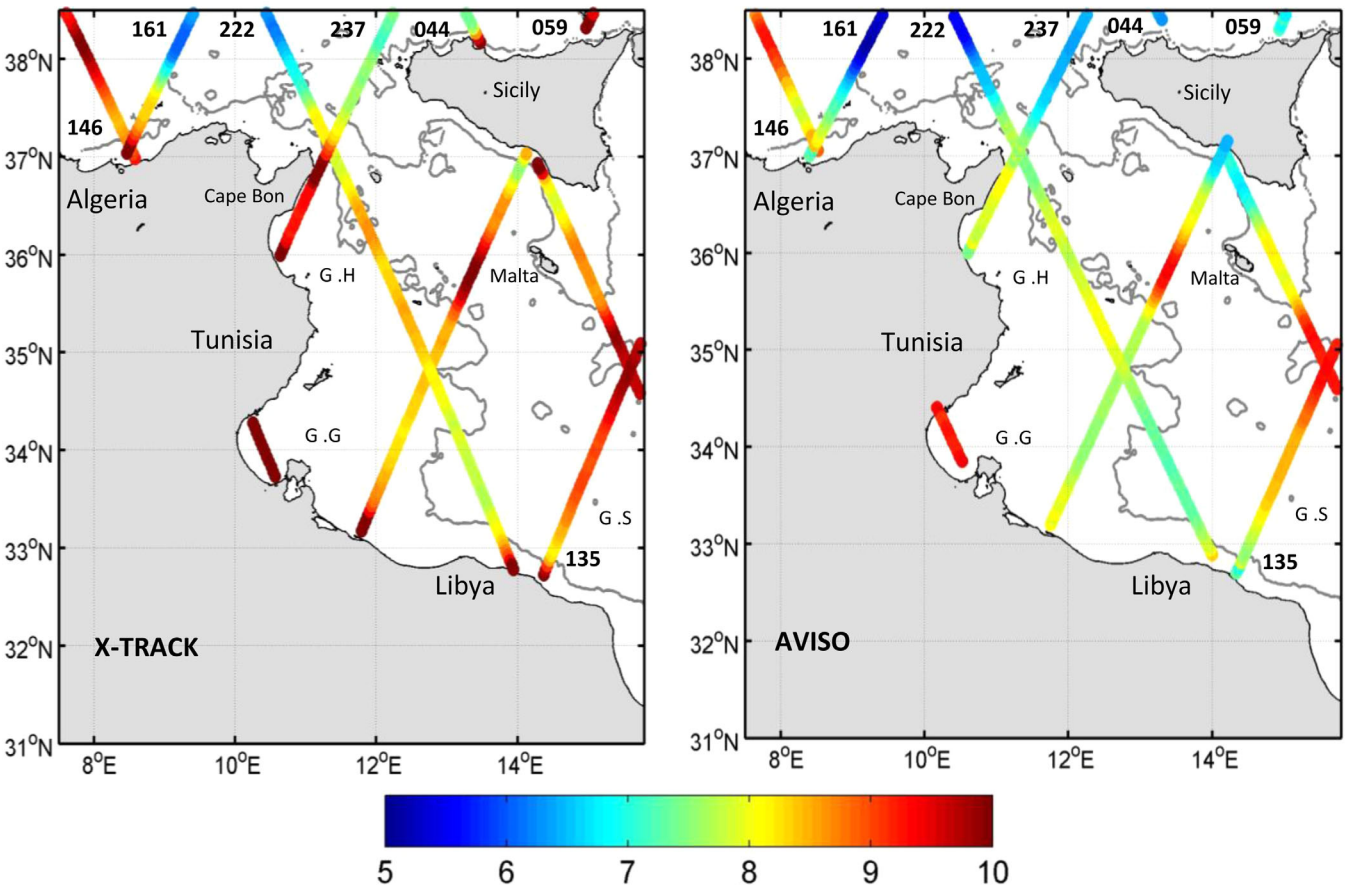

Figure 3. Maps of sea level anomaly standard deviation (in cm) of (left) X-TRACK and (right) AVISO from T/P+J1+J2 mission over the period 1993–2013. G.H is the Gulf of Hammamet, G.G is the Gulf of Gabes, and G.S is the Gulf of Sirte.

2.2. Estimation of Geostrophic Velocity

Altimeter-derived current velocities were obtained from along-track ADT assuming geostrophy. They represent estimates of the cross-track geostrophic component of the surface currents. The across-track geostrophic velocity anomaly V_g is given by:

$$V_g = \frac{g}{f}\frac{\Delta h}{\Delta x} \tag{1}$$

where g is the gravitational acceleration, f is the Coriolis parameter, and Δx and Δh are the distance and the difference in ADT between two adjacent data points along the track, respectively. *Powell and Leben* [2004] have shown that the altimetry instrument white noise generated internally can generate important errors in the estimation of mesoscale currents over the coastal oceans. Therefore, we used an optimal difference operator with weighted smoothing to minimize the noise impact when computing the across-track geostrophic velocity for the ADT:

$$\Delta pq = \sum_{n=-p}^{q} c_n \left(\frac{h_{i+n} - h_i}{n\Delta t}\right) \quad c_n \text{ are the weighting coefficients satisfying : } \sum_{n=-p}^{q} c_n = 1 \tag{2}$$

where h_i is the ADT at the current point "i," Δt is the sampling interval in seconds, p and q are the number of points before and after the current point, and N is the sum of p and q. Here Δh is smoothed by the optimal filter of *Powell and Leben* [2004] at a four-point size (i.e., 25 km; $p = 2$, $q = 2$). *Liu et al.* [2012], *Bouffard et al.* [2010] *Deng et al*, [2008], and *Powell et al.* [2006] have already used a similar filter for coastal ocean studies over areas characterized by a small baroclinic Rossby radius of deformation. Use of the filter is expected to result in a slope noise standard deviation of 2–4 cm/s in the geostrophic velocity fields [*Powell and Leben*, 2004].

We also computed the meridional and zonal geostrophic velocity anomalies at monosatellite crossover points. At crossover points, we have two components of geostrophic velocity from each altimetric track, V_1 and V_2 for the ascending and descending passes, respectively. The known angle α between the ground tracks and the north meridian varies only as a function of latitude. The residual velocity can then be computed in any orthogonal projection; for the current case, we computed the east/south components (U,V) following *Parke et al*. [1987] and *Morrow et al*. [1994]:

$$U=\frac{V_1+V_2}{2\cos\alpha} \qquad V=-\frac{V_1-V_2}{2\sin\alpha} \tag{3}$$

A discussion of the errors associated with the geometric transformation in a monosatellite crossover configuration can be found in *Morrow et al*. [1994].

2.3. Ancillary Data

2.3.1. Current Meter Data

The mooring (C02 on Figure 1) is located in the western sill of the Tunisia-Sicily Channel. The station is equipped with an upward-looking ADCP to monitor the upper part of the water column, three point-wise current meters in the lower layer and an autonomous CT probe at 100 m above the seafloor. Because we were interested in the near-surface layer for comparisons with altimetry data, only the ADCP data were considered. The reader is referred to *CNR IAMC and CNR ISMAR* [2009] for further technical information on quality control and editing procedures. The ADCP data used in this study were available for 286 days from April 2003 to January 2004. The near-surface velocity components (the top bin at 26 m below the surface) were 48 h low-pass filtered to discard the high-frequency fluctuations.

2.3.2. Tide Gauge Records

Three tide gauge stations, all located along the Tunisian coast, were selected because of their proximity to satellite ground tracks: Kelibia, Sousse and Lampedusa (see Figure 1 for their locations). Lampedusa tide gauge data were extracted from the PSML database (Permanent Service for Mean Sea Level, http://www.psmsl.org/data/obtaining/). Only monthly averaged measurements [*Holgate et al*., 2013] were available from 2002 to 2013. For the Kelibia and Sousse stations, hourly tide gauge records were provided by the IHE (Ingénierie de l'Hydraulique de l'Equipement et de l'Environnement, rafik-ihe@planet.tn), spanning the time period from February to May 2005. To make in situ sea level as consistent as possible with the corrected altimetry elevations, the tidal signals were filtered from the hourly tide gauge observations using harmonic analysis based on the T-Tide method described in *Pawlowicz et al*. [2002]. The dynamic atmospheric correction applied to altimetry data was also removed using the same correction, i.e., a combination of the barotropic MOG2D model, *Carrère and Lyard* [2003] and the inverse barometer formula. Note that the tides are well resolved by the MOG2D model. For this study, we considered that the high-frequency signals corresponding to tides and to the dynamic atmospheric correction were already filtered in the monthly Lampedusa sea level time series. Concurrent time series from tide gauges and altimetry SLA were finally obtained by removal of the mean sea level value computed over the same time period.

2.3.3. Sea Surface Temperature (SST)

Two kinds of SST products were used to analyze the features highlighted by the altimetric geostrophic currents and to provide complementary information on the ATC system surface patterns. With respect to the mesoscale variability, we first considered a regional daily Level 3 product at a high spatial resolution (1/16°) representative of night SST values obtained from the MyOcean project (www.myocean.eu.org/) [*Buongiorno Nardelli et al*., 2013] and made available since 2012. The individual SST maps were selected in accordance with the altimetry along-track availability in cloud free conditions. In section 4, we compute a monthly SST climatology from a sequence of Advanced Very High Resolution Radiometer (AVHRR) composite images (with a spatial resolution of 1.1 km, and temperature resolution of 0.012°C) made available by the DLR EOWEB-Earth Observation Information Service (http://eoweb.dlr.de). The time series data set covers the period of 1998–2007 and was generated from NOAA images using a weekly compositing period.

3. Comparison Between Altimetry and External Observations

3.1. Comparison With Tide Gauge Data

It was shown in section 2.1 that significant differences were observed between AVISO and X-TRACK products, both in terms of data availability and SLA standard deviation. The next step was to assess the quality

Table 1. Average Statistics of Altimetry Data Located Within 60 km (~3 and 21 km) From the Available Tide Gauge (Moored ADCP) Stations[a]

In Situ Station/ Type of Instrument	Altimetry Tracks	Altimetry Product/ Parameter	Number of Altimetric Data	Number of Samples	Standard Deviation	Root-Mean-Square Difference	Correlation at 95% Significance Level
Lampedusa/TG	059, 222	X-TRACK/SLA	30	127	7.52 (8.15) cm	5.28 cm	0.775
		AVISO/SLA			6.98 (8.15) cm	5.23 cm	0.770
Kelibia/TG	222, 237	X-TRACK/SLA	32	9			
		AVISO/SLA	30				
Sousse/TG	222, 237	X-TRACK/SLA	5	9			
		AVISO/SLA					
All stations/TG	059, 222, 237	X-TRACK/SLA	67	145	5.42 (6.64) cm	5.06 cm	0.650
		AVISO/SLA	65		4.66 (6.64) cm	4.93 cm	0.635
C02/Moored ADCP	222	X-TRACK/AGV	1	28	10.38 (10.50) cm/s	10.90 cm/s	0.50
		AVISO/AGV			12.07 (10.50) cm/s	13.82 cm/s	0.45
	237	X-TRACK/AGV	1	28	9.78 (12.02) cm/s	8.05 cm/s	0.79
		AVISO/AGV			10.19 (12.02) cm/s	8.24 cm/s	0.77

[a]TG is Tide Gauge, SLA is Sea Level Anomaly, and AGV is Absolute Geostrophic Velocity. The value between parenthesis indicates the standard deviation of the in situ time series. The number of altimetric data is the number of altimetric data used within a 60 km distance from the TG. The length of the altimetric time series is the number of samples.

of these altimetry data sets in the study area and to determine which one provides the best information according to our scientific objectives. For this purpose, AVISO and X-TRACK sea level anomaly time series (from tracks 059, 222, and 237) were compared with concurrent tide gauge observations (see Figure 1 for their locations). For each tide gauge station, we considered all the altimetric points located within a 60 km radius and computed the standard deviations, the root-mean-square of the differences and correlation coefficients between the tide gauge and altimetry SLA time series. Kelibia and Sousse tide gauge data are hourly observations and cover a ~3 month period corresponding to only nine TP+J1+J2 repeat cycles. Lampedusa data correspond to a 12 year monthly time series (127 samples). In the first case, the tide gauge time spans closest to the altimetry observations were considered, whereas in the second case, altimetry observations were monthly averaged before the statistical computation. Table 1 synthesizes the mean results obtained from altimetry for Lampedusa tide gauge station. On average, X-TRACK has slightly more altimetry reference points located in the tide gauge neighborhood (see "Number of altimetric data" in Table 1) and

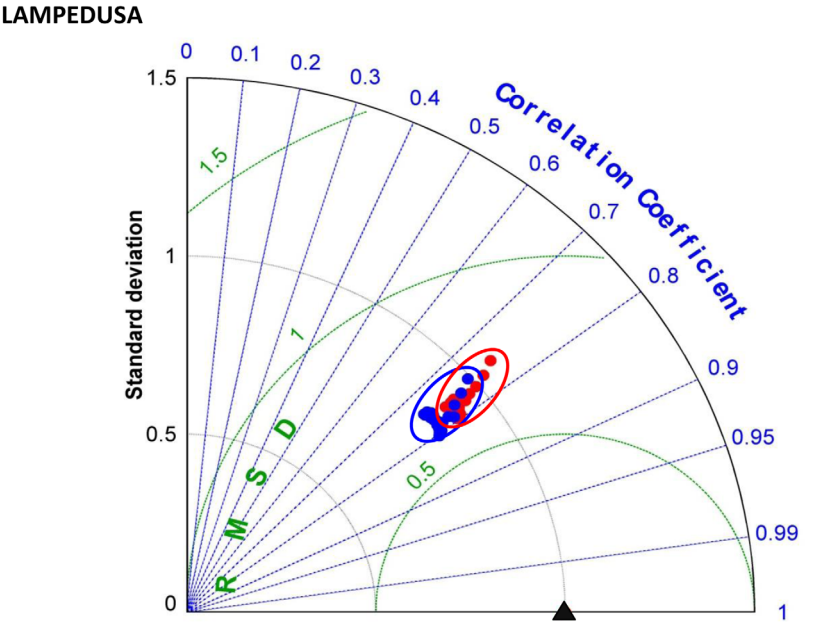

Figure 4. Normalized Taylor diagrams of Lampedusa tide gauge station. The selected AVISO in blue and X-TRACK in red data are within 60 km radius of each tide gauge.

exhibits slightly better correlations. As was already observed in Figure 3, AVISO standard deviations are lower (∼8 cm in average) and show a lower mean root-mean-square difference than X-TRACK, meaning that the X-TRACK data set exhibits an improved percentage of variability explained at the tide gauge station.

To complement the previous analysis, Taylor diagrams [*Taylor*, 2001] provide a way of representing all the statistics on the same graph, which more easily illustrates how closely altimetry data matches the information provided by tide gauge observations (see Figure 4). For this study, the Lampedusa tide gauge in situ data represent the "reference" field and the two altimetric along-track SLA products (AVISO and X-TRACK) are the "test" fields. Statistics obtained for each individual altimetry point located within a 60 km radius from the tide gauge is represented by a triangle or a dot. The green contours indicate the root-mean-square differences between the altimetry and the in situ SLA. The correlation coefficients and standard deviations are shown on the dashed blue lines and black arcs, respectively. Comparisons at the Lampedusa tide gauge (Figure 4) show good agreements with altimetric data for both AVISO and X-TRACK (correlations between 0.7 and 0.8). These good results are due to the monthly low-pass filtering, which reduces noise and part of the short-term variability.

In Figure 5, the SLA time series at the altimetry point showing the highest correlation values are compared with the corresponding tide gauge data (black curve) for both X-TRACK (in red) and AVISO (in blue). The locations of these observations are indicated in the right part of Figure 5. Note first that X-TRACK data with maximal correlation are systematically closer to the tide gauge stations than the AVISO data (23 km instead of 59 km in the case of Lampedusa), which is similar to the results obtained by *Bouffard et al*. [2011] over the northwestern Mediterranean. The correlations are also significantly higher, which shows a better consistency between the Lampedusa tide gauge observations and the coastal SLA data provided by X-TRACK than by AVISO. The obtained statistics for Sousse and Kelibia are not shown because of the short time series (nine samples). However, their time series (black lines, Figures 5b and 5c) show relative better agreement with the corresponding X-TRACK pattern (red lines, Figures 5b and 5c) than the AVISO one (blue lines, Figures 5b and 5c). In addition to errors associated with processing of both altimetry data sets, part of the incoherence between altimetry and tide gauge signals is likely because of the nonexact collocation between the observations, which do not exactly sample the same local dynamic systems.

3.2. Comparison With Moored ADCP Observations

To assess the accuracy of the altimetry-derived geostrophic current, we computed absolute geostrophic velocity (AGV) from both the AVISO and X-TRACK ADT. The AGVs were then compared to the moored ADCP velocities in the across-track direction. The C02 across-track in situ velocity was low-pass filtered using a 48 h cutoff frequency. The ADCP velocity vector was then rotated into the across-track and along-track directions of the satellite pass. Fortunately, the mooring is located on the T/P+J1+J2 satellite ground track 237 and is in the vicinity of T/P+J1+J2 track 222 (Figure 1). Following *Liu et al*. [2012], we considered the closest altimeter point on each track (∼3 km for track 237 and ∼21 km for track 222) from the moored ADCP location. The altimeter AGVs were then averaged among the six adjacent points to further reduce the effects of small-scale features [*Liu et al*., 2012].

For both AVISO and X-TRACK data, the time series of across-track geostrophic velocities derived from altimetry are in good general agreement with the concurrent ADCP measurements (Figure 6). Corresponding statistics are provided in Table 1. For track 237, the root-mean-square difference between the altimeter-derived and moored velocity anomalies is 8.24 cm/s for AVISO and 8.05 cm/s for XTRACK. For track 222, the corresponding values are 13.82 and 10.9 cm for AVISO and X-TRACK, respectively. The standard deviation of the velocities for both altimetric products are consistent with those from current meter data. However, those from X-TRACK (track 222) are better matched. Given the expected level of 4–6 cm/s, errors associated with the optimal filter [*Powell and Leben*, 2004] and the root-mean-square of the differences of ∼6 cm/s obtained for the deep oceans [e.g., *Strub et al*., 1997], the obtained results of 8–10 cm/s are encouraging and perfectly in line with other coastal altimetry studies [*Vignudelli et al*., 2005; *Bouffard et al*., 2008; *Le Hénaff et al*., 2011; *Liu et al*., 2012]. Both products should allow retrieval of relevant dynamic information over the Tunisian shelf; however, the use of X-TRACK data leads to slightly better statistics than the use of AVISO data.

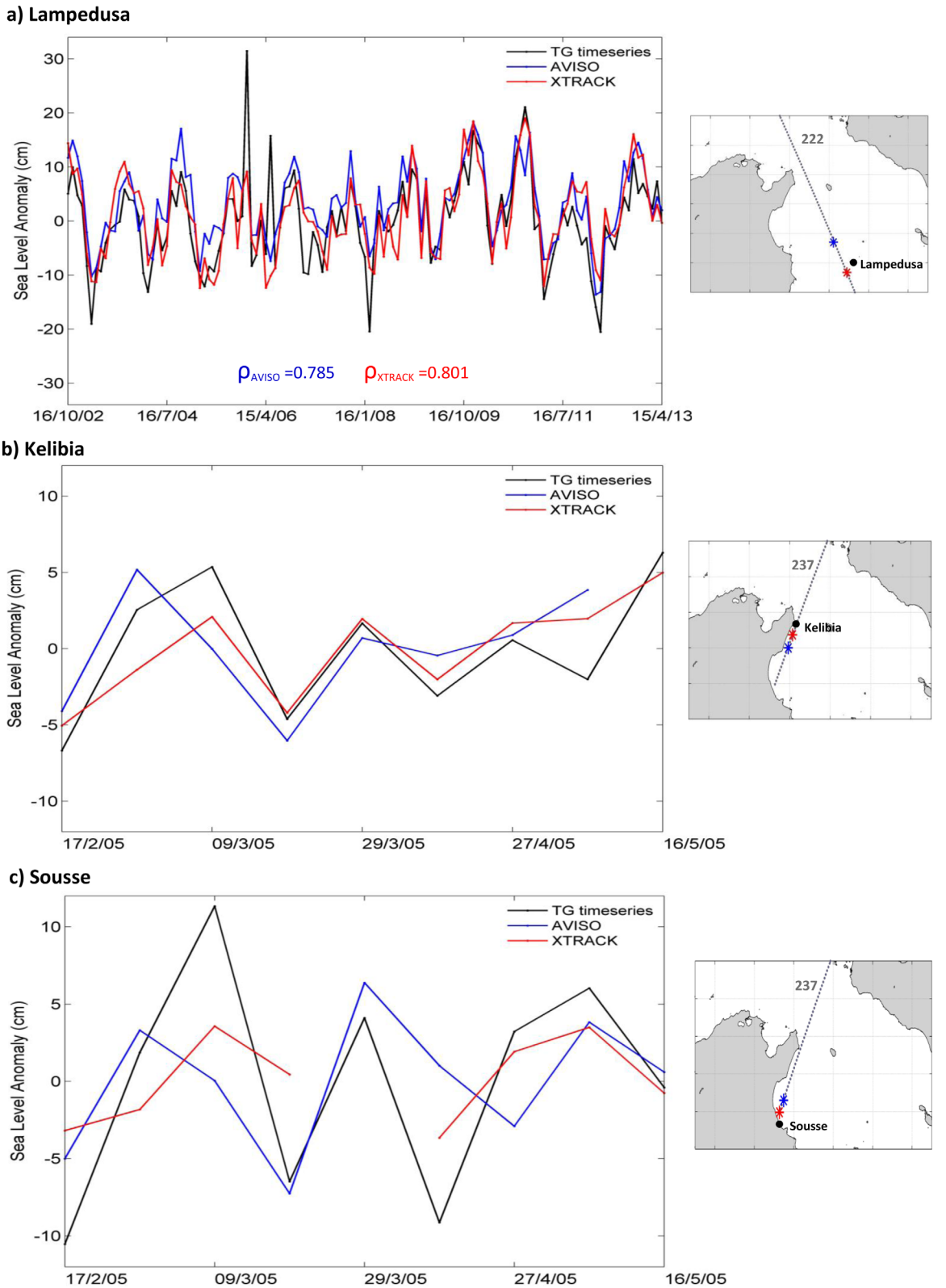

Figure 5. Tide gauge (black line) time series versus X-TRACK (red line) and AVISO (blue line) time series of the altimetry data point with the highest correlation coefficient. The positions of tide gauge stations (black dots) and the corresponding X-TRACK (red star) and AVISO (blue star) data are shown on the map at the right of each plot. "ρ" is the correlation coefficient of altimetry with tide gauge time series.

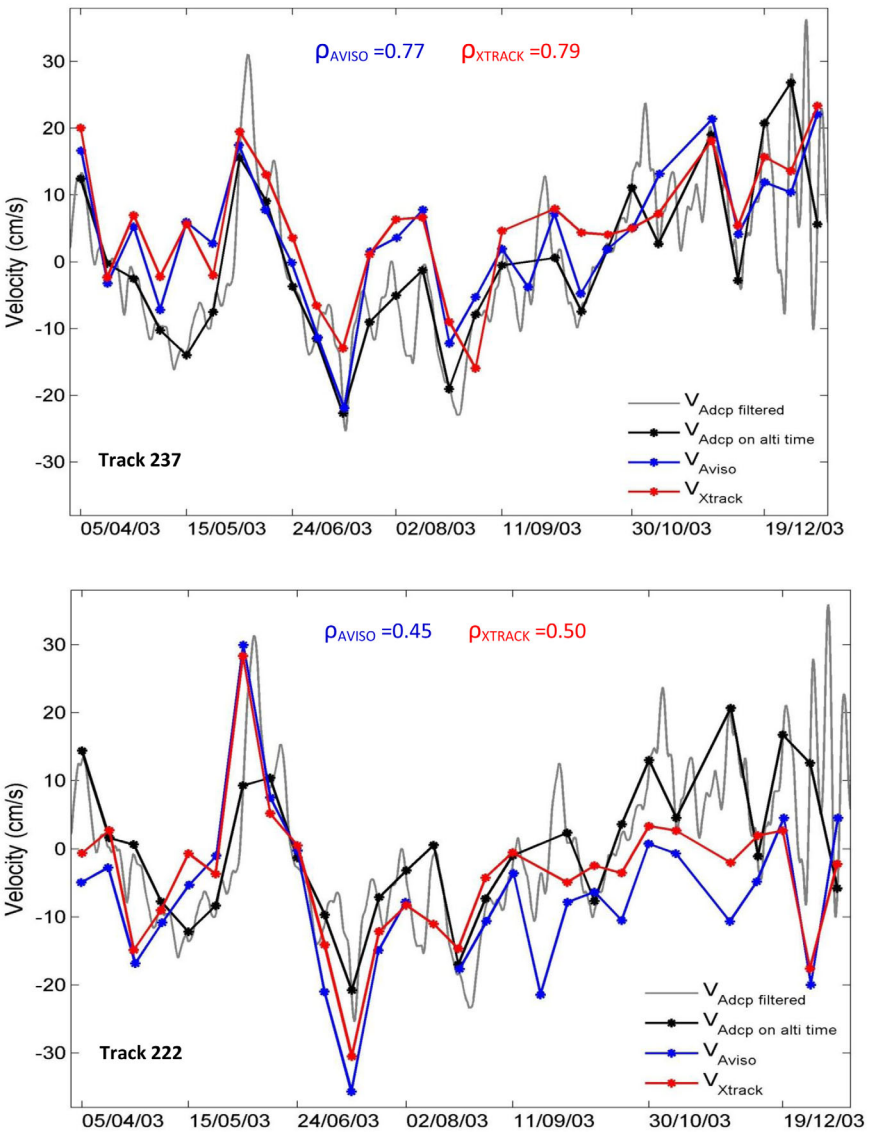

Figure 6. Comparison of velocity time series of X-TRACK (red line) and AVISO (blue line) for tracks (top) 237 and (bottom) 222 with ADCP (black line) data. Positive velocities correspond to the North East and South East directions for tracks 222 and 237, respectively. The 48 h low-pass filtered ADCP time series is overlaid in grey.

3.3. Qualitative Comparisons With Satellite SST Fields

In addition to in situ data, high-resolution SST daily images were used to assess the consistency of the altimetric AGV with respect to thermal frontal structures. The study area is dominated by mesoscale dynamics associated with short temporal scales ranging from 1 day to a week and to spatial scales of a few tens of kilometers, making the use of a low-level SST product more relevant than use of the smoothed high-level products. We used relatively cloud-free SST daily maps that coincided with the TP/J1/J2 passes. Two examples are presented in Figure 6, which shows coherent structures (i.e., fronts, filaments, and mesoscale eddies) in SST fields and altimetry-derived AGVs.

On 6 November 2012, the main SST feature is a marked thermal front separating cold waters (globally originating from the Algerian basin) from warmer waters of eastern basin origin that spread over the Tunisian/Libyan shelf (top of Figure 7a). Both altimetry-derived AGV products reveal coherent structures with front undulations along the 059 track, with alternating SE/NW flows and a well-marked anticyclonic swirling of colder waters in the central Tunisia-Sicily Channel (13°E and 35.5°N). X-TRACK has generally stronger amplitude and a better sampling than AVISO, particularly inside the Tunisia-Sicily Channel and near Sicily, where

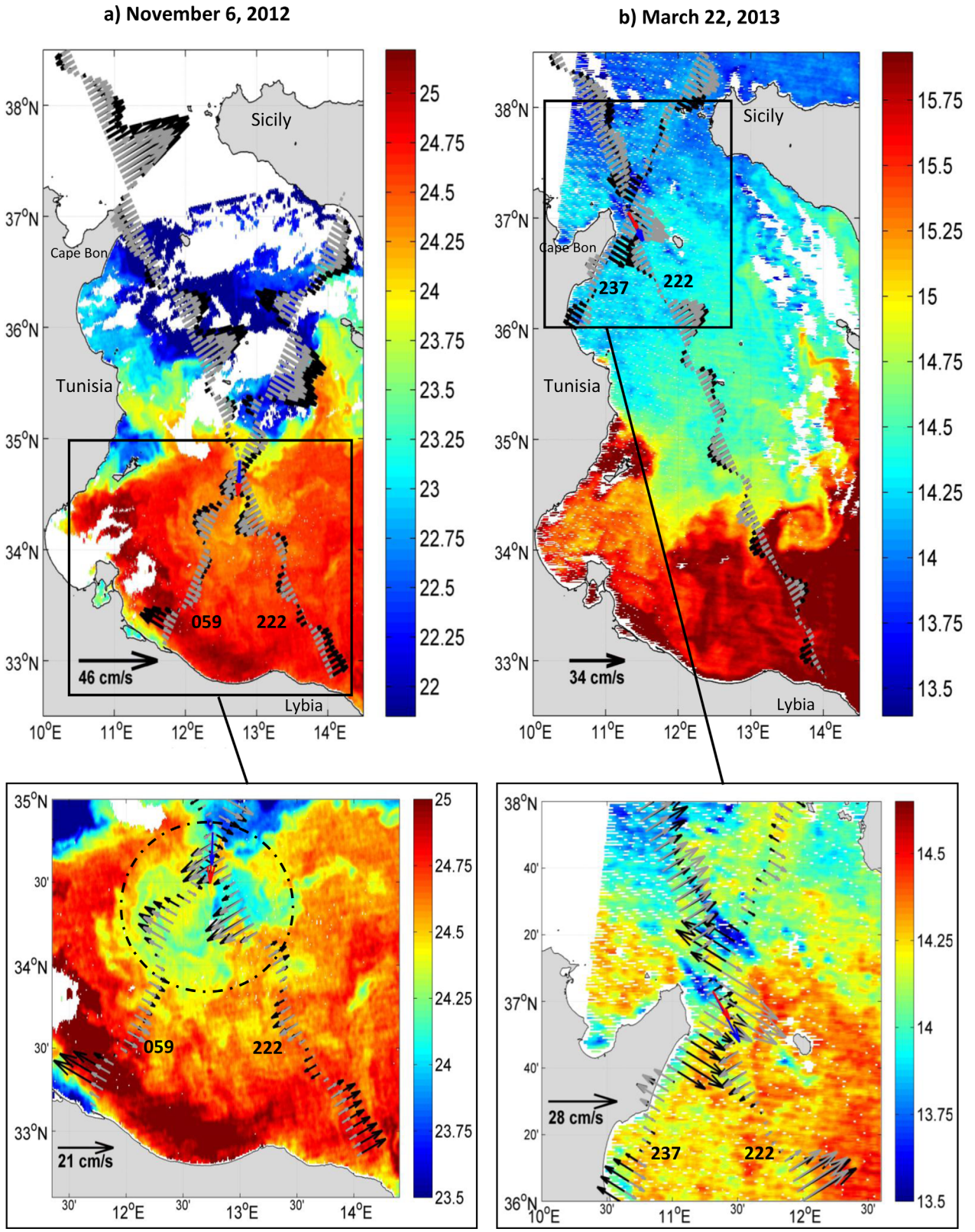

Figure 7. Comparisons of SST (in °C) with X-TRACK (black) and AVISO (grey) crosstrack velocities over (top) the Tunisia shelf with zoom (bottom) over the Gulf of Gabes and Cape Bon-Sicily. X-TRACK (AVISO) velocities at crossover locations are in red (blue) and are computed for (a) from track 059 (6 November) and track 222 (3 November). Dashed circles highlight mesoscale anticyclonic eddy. The SST pattern is derived from MyOcean products with 1/16° resolution.

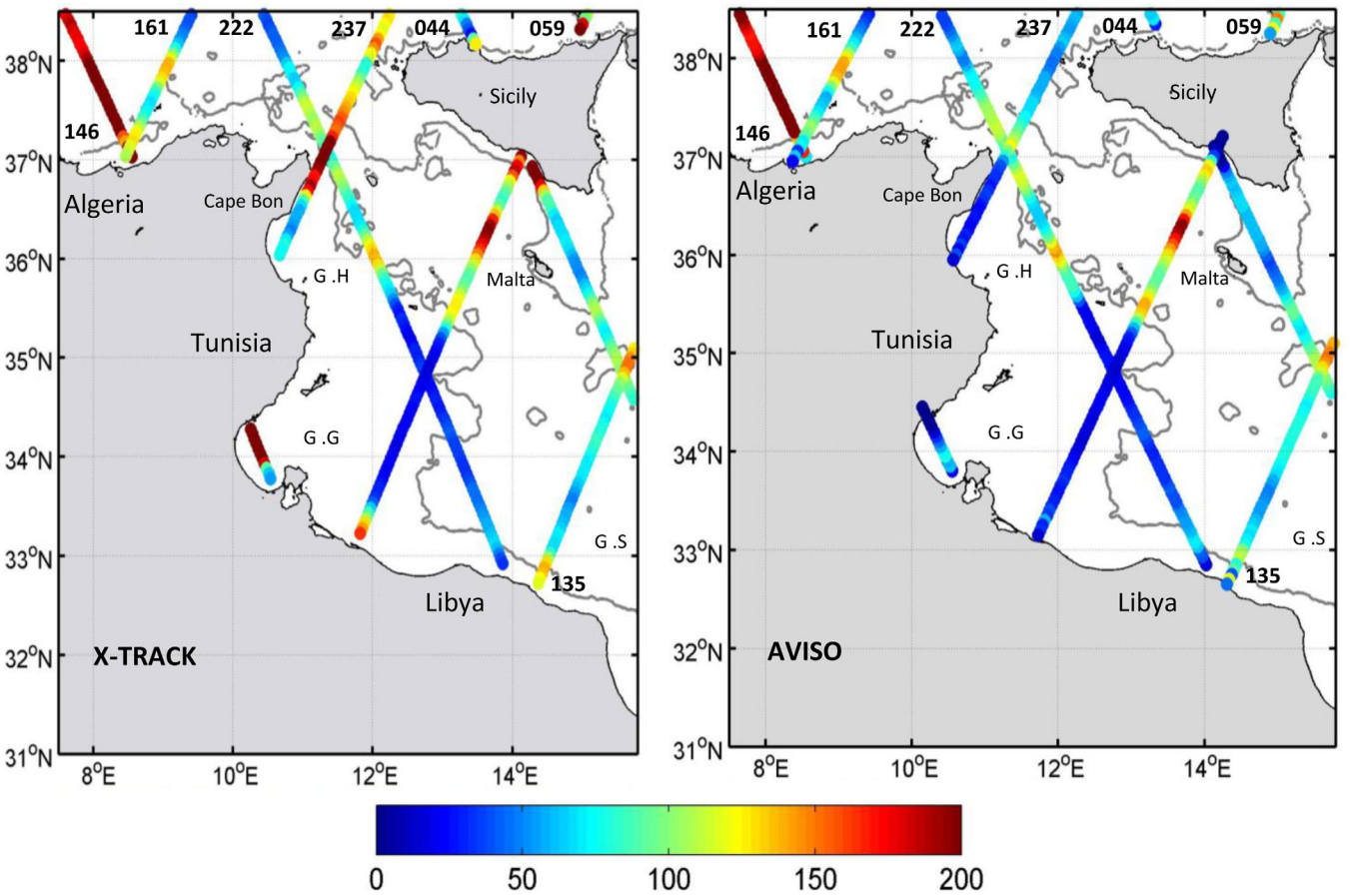

Figure 8. Variance of (left) X-TRACK and (right) AVISO crosstrack velocities as a proxy for EKE (in cm^2/s^2) over the period 1993–2013. G.H is the Gulf of Hammamet, G.G is the Gulf of Gabes, and G.S is the Gulf of Sirte.

X-TRACK AGVs are more consistent with the southeast cold inflow corresponding to the AIS signature. In the Gulf of Gabes, the qualitative coherence between mesoscale structures captured by SST and altimetry is less obvious because of the presence of more homogeneous warm waters, but a zoom (bottom of Figure 7a) confirms that mesoscale AGV variability is still associated with concurrent SST patterns: a patch of relatively colder water swirling anticyclonically on the outer shelf and a coastal flow of warmer water from the Libyan shelf in the south-most part. For the latter pattern, the X-TRACK-derived velocities are clearly greater than the AVISO ones and thus correlate better with the SST pattern.

The second example (Figure 7b), on 22 March 2013, shows a less marked north/south thermal front but suggests a greater spreading of Atlantic Water from the Algerian basin throughout the Tunisian shelf. The altimeter track crossing the Tunisia-Sicily Channel (track 222) is roughly in the direction of the main flow (i.e., the ATC or AIS). Consequently, the main current patterns are of lower amplitude than the ones previously observed. Both SST structures and altimetry-derived currents suggest the presence of eddy-like turbulent exchanges along the track 222 path (which approximately follows the 200 m isobath down to the Libyan shelf). This second example also shows a crossover with track 237 at the entrance of the Tunisia-Sicily Channel (bottom of Figure 7b). Some differences exist between the two altimetry-derived products regarding the position of the Atlantic Water inflow near Cape Bon and the presence of an eddy-like pattern located a few kilometers northward on the X-TRACK data. The resulting absolute currents at the crossover point are in the same SE direction, which agrees with previous studies on ATC current position along the 200 m isobaths.

The higher variability of the X-TRACK-derived currents is illustrated in Figure 8, where the variance of the AGV is used as a proxy of the Eddie Kinetic Energy (EKE). The EKE increases twofold at the entrance of the Tunisia-Sicily Channel near Cape Bon, south of Sicily (tracks 059 and 044), and on the Tunisian and Libyan

Shelf (tracks 059 and 135), ranging from 150 to above 200 cm^2/s^2 for X-TRACK. These are very consistent results in light of the EKE estimated from drifter observations (over 1990–1999) [*Poulain and Zambianchi*, 2007], which reached values of 225 cm^2/s^2 along areas of the Algerian Current, ATC, AIS, and the southern Ionian near Libya in winter (along areas of the Algerian Current and AIS in summer). Between Pantelleria and Malta, the EKE reaches 290 and 360 cm^2/s^2 in summer and winter, respectively, as shown in *Poulain and Zambianchi* [2007]. Moreover, EKE estimates based on numerical modeling (over 2008–2010) [*Sorgente et al*., 2011] led to large fluctuations, higher than 100 cm^2/s^2 in regions with strong currents (the AC and AIS) and up to 350 cm^2/s^2 [*Sorgente et al*., 2011]. Here the underestimate of the EKE proxy from altimetry is due to the different sampling periods and to the fact that along-track altimetry resolves only one direction of the geostrophic currents.

At this stage, we can confirm that both regional altimeter data sets are in good agreement with several independent observations. These agreements are however more obvious in X-TRACK than in AVISO; X-TRACK shows more variability as well as better statistics and an increased coverage over the coastal domain. Therefore, the seasonal variation of the regional circulation will be further discussed from the single X-TRACK data set. First, we will focus on the general seasonal characteristics of the circulation. Then, we will analyze the boundary currents in more detail. Finally, we will propose a new schematic description of the seasonal circulation from altimetry.

4. Seasonal Evolution of the Regional Circulation

4.1. General Characteristics Observed From Altimetry

Unlike available in situ observations in the study area, the long period of altimetric observations allows for the separation of the seasonal variability of the surface circulation from the mesoscale/inter-annual variability. To do this, we applied the method already used in *Birol et al*. [2010] over the northwestern Mediterranean Sea. We computed a monthly climatology of AGV over the period 1993–2013, and we then analyzed the mean current pattern along with its absolute amplitude "A" (Figure 9, top). "A" is defined as the difference between the extrema velocity values obtained (maximum minus minimum). The months during which the maximum (Figure 9, bottom right) and minimum (Figure 9, bottom left) values of "A" were observed provide information on the temporal characteristics of the variability of the seasonal currents. The results globally confirm the seasonal circulation features highlighted in previous studies based on shorter time series of in situ data, satellite imagery observations, or numerical modeling.

The first main circulation pattern observed is the large eastward vein (>30 cm/s) with significant values of "A" (>15 cm/s) at the edge of the Tunisian/Algerian coasts (tracks 146 and 161 at 37°N–38°N), where the Algerian Current is expected to be energetic [*Millot*, 1999]. It reaches track 222 (at 37°N–38°N) with the same intensity. However, its continuation on track 237 is somewhat confusing as the latter clearly shows two current veins. This suggests a separation of two branches, the first in the southern part of the Tunisia-Sicily Channel near Cape Bon and the second near the western Sicily coast. The separation, which occurs on the western flank of Adventure Bank, is likely due to bathymetric constraints. The northward Algerian Current branch would feed both the AIS and the northeast flow observed on track 044 north of Sicily (the Bifurcation Tyrrhenian Current, as stated by *Sorgente et al*. [2011]). However, the southward Algerian Current vein would feed the ATC. Near Cape Bon and the western Sicily coast, the amplitude of the seasonal cycle and the southeastern mean current vectors are also strong. This corresponds to the ATC (along the track 237: 36.9°N–37.4°N and track 222: 36.7°N–37°N) and the AIS (along the track 222: 37.3°N–37.8°N and track 237: 37.8°N–37.9°N) positions as observed in *Ciappa* [2009] and *Lermusiaux and Robinson* [2001].

South of Cape Bon, along track 222, the mean eastern AGVs are low, but several undulations with significant amplitudes (from 10 to above 15 cm/s) suggest a reversal of the current directions. At the central part of the Tunisia-Sicily Channel, the South East mean current on track 059 (35.2°N–35.3°N) seems to shift South West afterward on track 222 (34.1°N–34.2°N) with an amplitude above 11 cm/s. This matches the ATC path steered by the 200 m isobath [*Alhammoud et al*., 2004; *Ciappa*, 2009]. Moving east to the Malta Channel (along the track 059: 36°N–37°N and track 044: 35.5°N–36.3°N), the large eastward undulations and high amplitudes (10–15 cm/s) observed are likely the signature of the AIS flowing toward the Ionian Basin [*Sorgente et al*., 2011].

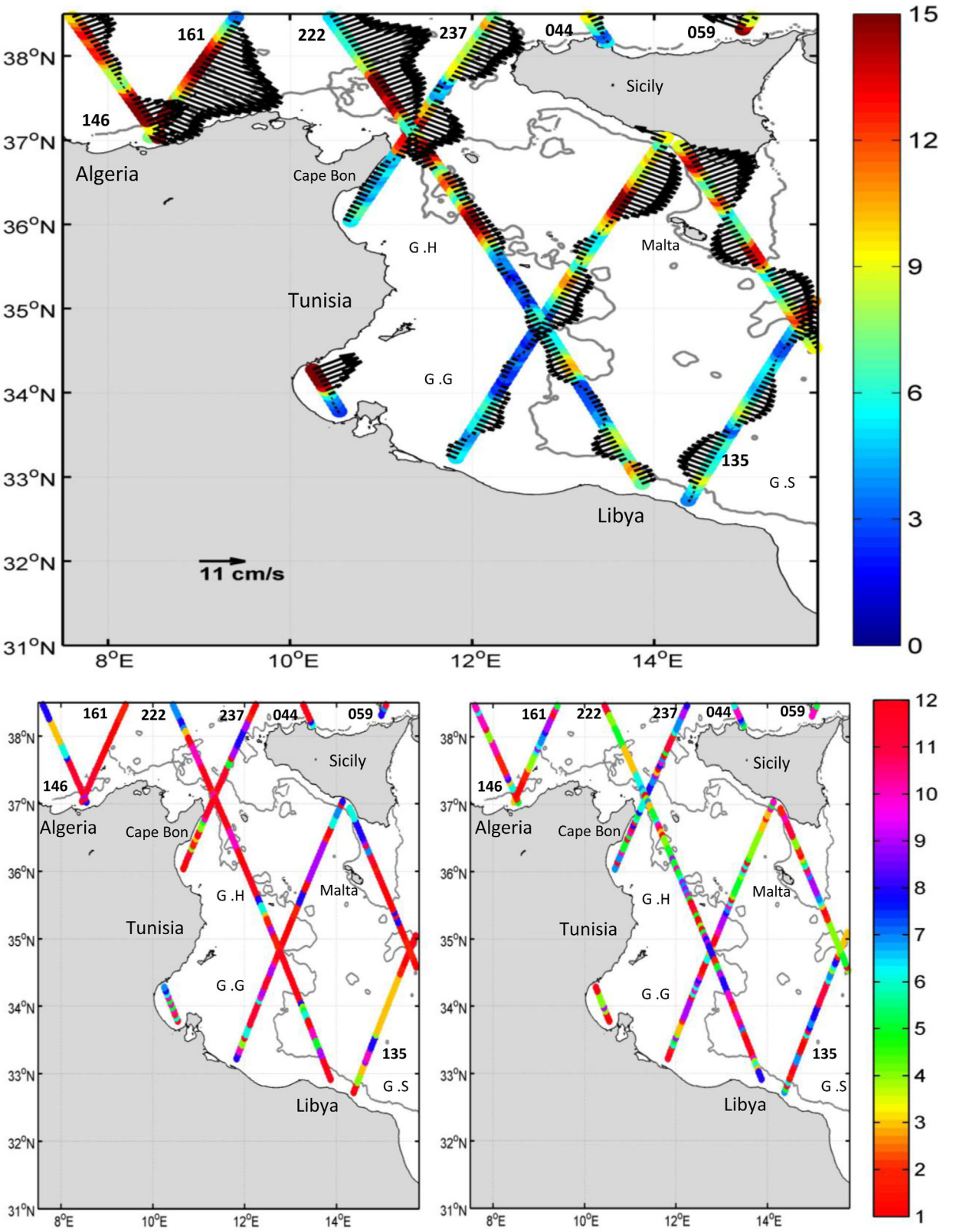

Figure 9. (top) Amplitude in cm/s and phase of (bottom right) maximum and (bottom left) minimum in month number observed in the current seasonal cycle derived from X-TRACK. The 200 m isobath (black solid line) is from the ETOPO2v1 global gridded database. G.H is the Gulf of Hammamet, G.G is the Gulf of Gabes, and G.S is the Gulf of Sirte.

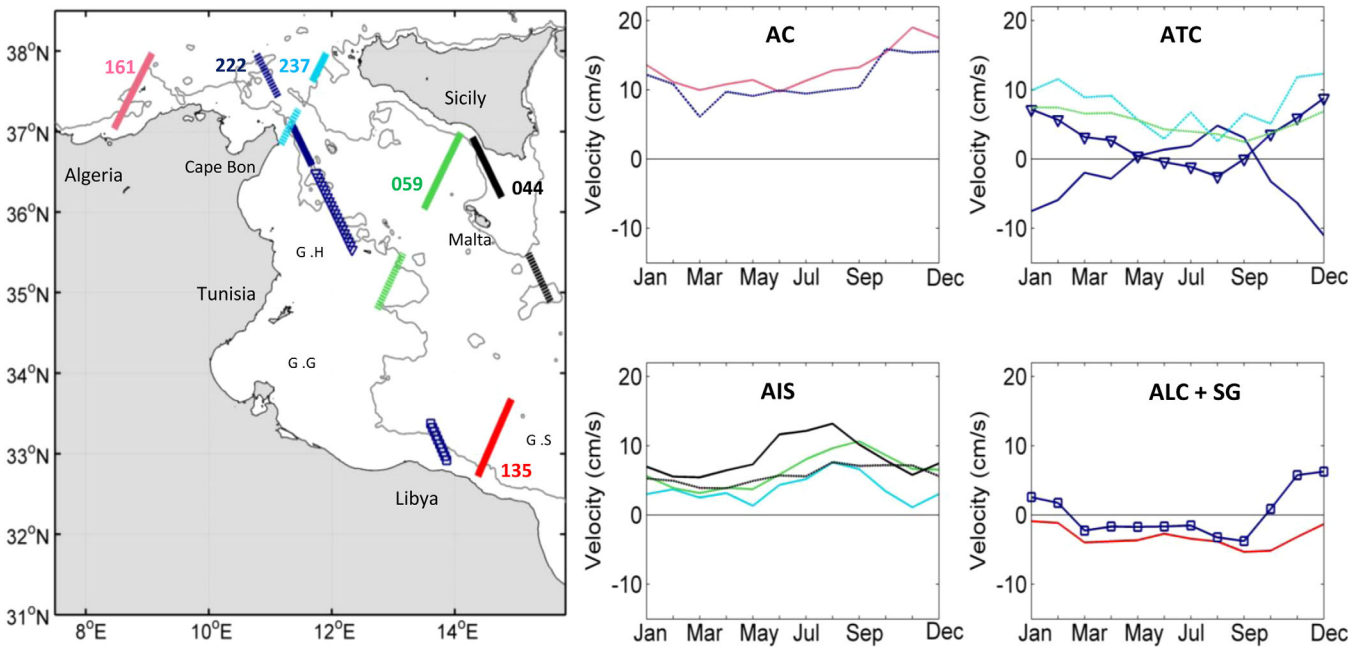

Figure 10. (top right) Spatially averaged AGV time series over the (top left) AC, ATC, AIS, and ALC/SG paths in the central Mediterranean. AC is the Algerian Current, ALC is the Atlantic Libyan Current, and SG is the Sidra Gyre. The 200 m isobath (grey solid line) is from ETOPO2v1 global gridded database. G.H is the Gulf of Hammamet, G.G is the Gulf of Gabes, and G.S is the Gulf of Sirte.

Further south on track 135, the large reversal of the AGVs (from South East to North West) off the Libyan shelf (between 14.5°E–15.5°E and 33°N–34.2°N) potentially corresponds to the Sidra Gyre, a relatively large (diameter of 150–200 km) anticyclonic permanent eddy characterized in previous studies as the main dynamic mechanism influencing the seasonal Atlantic Water outflow outside the Tunisia-Sicily Channel [*Gerin et al*., 2009; *Ciappa*, 2009; *Sorgente et al*., 2011; *Poulain and Zambianchi*, 2007]. The Sidra Gyre shows lower amplitudes (5–8 cm/s) than the upper ATC and AIS veins. However, "A" increases correspondingly along the tracks 222 and 135 (approximately 33°N), reaching 12.5 and 9 cm/s, respectively. This might correspond to a branch of the ATC that shifts southward toward the Tunisian/Libyan shelf and connects with the Atlantic Libyan Current, as observed in *Sorgente et al*. [2011].

The AIS related veins (on tracks 237, 059, and 044) show a maximum in summer. The northern part of the Sidra Gyre (on track 135) is maximum in early spring but the period of the maximum is unclear on its southern part. Over most of the remaining areas, the maximum amplitude is clearly reached in winter. However, the corresponding minimum phase displays a larger dispersion over the region (ranging from June to September) than the maximum. This does not allow full characterization of the corresponding seasonal cycles. To complete the analysis, we will use time series of spatially averaged AGVs (Figure 10) where tracks cross the main current veins (Algerian Current, ATC, AIS, Atlantic Libyan Current and Sidra Gyre) identified above. Moreover, the seasonal variability of the circulation will also be discussed based on the climatological AGV patterns together with the corresponding SST fields (Figure 11) over 4 months. In fact, the Atlantic Water signature is known to be associated with a shelf slope density front [*Hamad et al*., 2006; *Ciappa*, 2009]. The Atlantic Water is generally detectable in summer SST patterns as cold waters at the entrance of the Tunisia-Sicily Channel [*Ciappa*, 2009].

4.2. Subregional Analysis of the Seasonal Variability

4.2.1. The Algerian Current and Tunisia-Sicily Channel Inflow

The spatially averaged AGV time series over the Algerian Current path (pink solid and blue dashed lines, Figure 10) show a well-phased North East current over the climatological year with a maximum in early winter, which suggests a continuity of the flows from the Algerian to the Tunisian/Sicilian shelves. Moreover, the spatial structure of the cross-track/crossover velocities in Figure 11 shows a qualitatively good agreement with the SST fields despite the averaged climatological scale. Indeed, the well-marked (whatever the season) Algerian Current vein on the northern parts of tracks 161 and 222 (Figure 11) is associated with a thermal front separating warmer Atlantic Water flowing near the coast and colder Tyrrhenian waters further

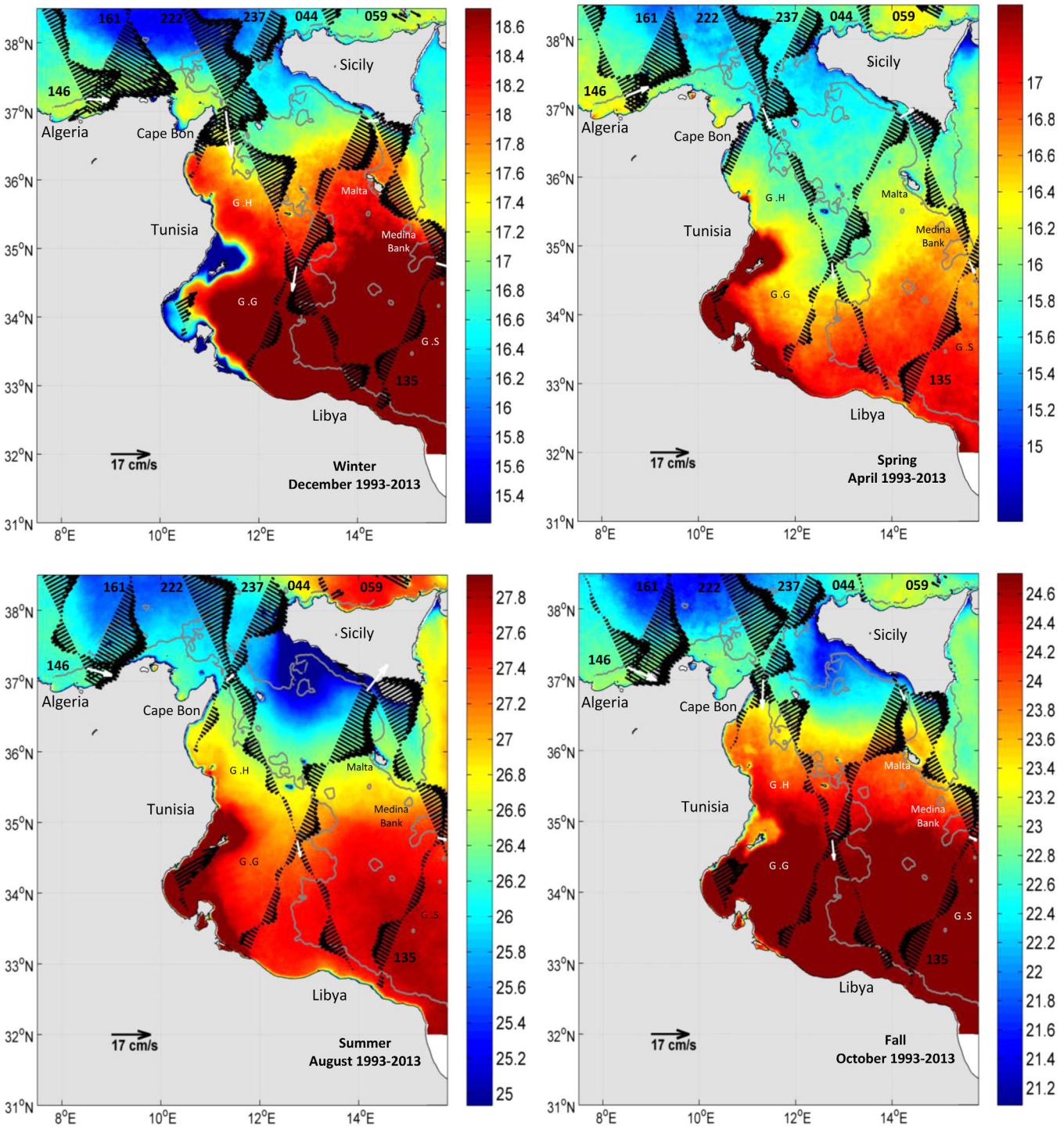

Figure 11. Maps of crosstrack (black) and crossover (white) geostrophic current from X-TRACK and SST over the climatological cycle. The 200 m isobath (grey solid line) is from the ETOPO2v1 global gridded database. SST data are from the DLH products with 1.1 km resolution. G.H is the Gulf of Hammamet, G.G is the Gulf of Gabes, and G.S is the Gulf of Sirte.

offshore. Moving southeast on track 237, part of the Atlantic Water is advected inside the Tunisia-Sicily Channel by the ATC and, at least partially, by the AIS/Bifurcation Tyrrhenian Current. The relative intensity of the two branches shows two opposite seasonal cycles with a southern ATC (northern AIS/Bifurcation Tyrrhenian Current) vein culminating in early winter (summer) as shown in the cyan dashed (solid) lines in Figure 10. Note that the resulting ATC branch is in phase with the Algerian Current seasonal cycle (cyan and blue

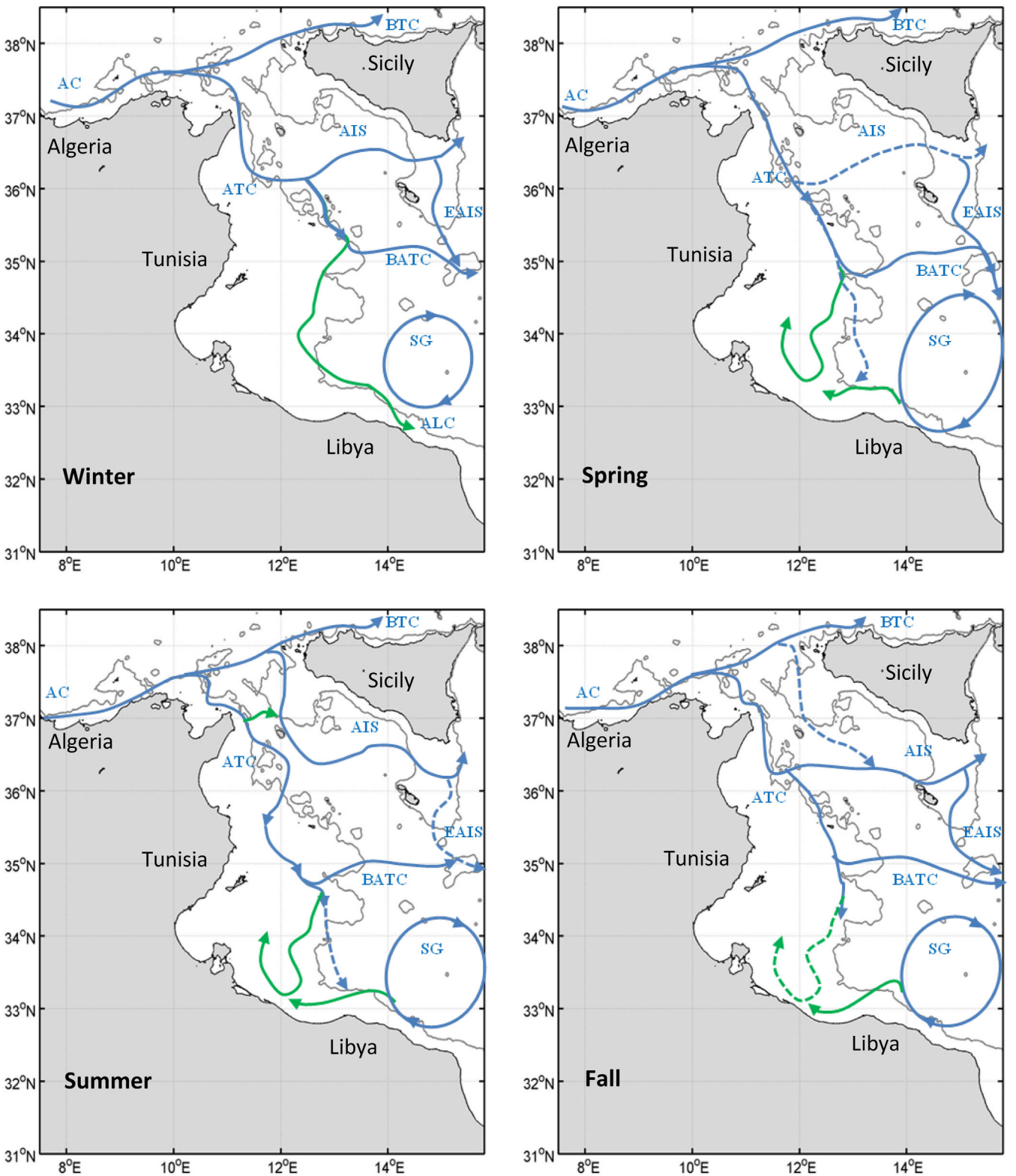

Figure 12. Seasonal circulation schemes in the central Mediterranean. The pronounced (suspected) branches are in solid (dashed) lines. The new (known) branches are in green (blue). From West to East—AC: Algerian Current, ATC: Atlantic Tunisian Current, BATC: Bifurcation Atlantic Tunisian Current, ALC: Atlantic Libyan Current, SG: Sidra Gyre, BTC: Bifurcation Tyrrhenian Current, AIS: Atlantic Ionian Stream, and EAIS: Eastern Atlantic Ionian Stream. The 200 m isobath (grey solid line) is from the ETOPO2v1 global gridded database.

dashed lines, Figure10). Over all the Tunisia-Sicily Channel, the cross-track AGVs (Figure 11) show the strongest values generally associated with the north/south thermal front of the Tunisia-Sicily Channel (i.e., between 32°N and 38°N). The latter is maximal (~3°C) in summer and decreases (~2°C) in winter.

4.2.2. The Atlantic Tunisian Current

The crossover AGVs of tracks 222-237 near Cape Bon (Figure11) confirm the seasonal variability of the ATC. Indeed, it is oriented more or less parallel to the 200 m isobath from fall to spring with intensities of 8–17 cm/s. However, the current intensity is weaker (4 cm/s) in summer and rather deviated northeastward, which reveals an inversion of the Cape Bon eastward flow (blue solid line, Figure 10) when reaching the Gulf of Hammamet (the blue triangle line, Figure 10). At the Gulf of Hammamet, the flow continues in a south-westward direction with a strongly decreasing intensity. Accordingly, the Atlantic Water would bifurcate in the Tunisia-Sicily Channel during summer into a weak ATC branch entering the Gulf of Hammamet and a stronger North East vein flowing toward Sicily and feeding the AIS. This suggests that most of the variability in the area is strongly steered by the bathymetry, except where the stratification is maximal in summer. The quasi-permanent southeast flow on track 059 (approximately 35°N and 12.5°E–13°E, Figure 11) confirms a preferential pathway of the ATC toward the Tunisian/Libyan shelf. Moreover, this permanent South East flow on track 059 (green dashed line, Figure 10) is moderately in phase with the upper ATC branch near Cape Bon (cyan dashed line, Figure 10). This confirms the predominant South East direction of the ATC and its early winter intensification already observed in *Gasparini et al*. [2007] and *Ciappa* [2009].

4.2.3. The Atlantic Libyan Current and the Sidra Gyre

Another interesting feature highlighted by Figure 11 is the possible signature of the Sidra Gyre on track 135 (approximately 33.5°N). This flow inversion is less marked in winter (red solid line, Figure 10), simultaneously with the ATC increase along the Tunisian-Libyan shelf (cyan dashed and blue square lines, Figure 10). The winter AGV also shows a coherent eastward flow over the southernmost part of tracks 222 and 135 (Figure 11) along the 200 m isobath. It is marked by high intensity (10 cm/s) and numerous small-scale undulations that indicate a complex eddy-like circulation at the source of mixing between the ATC and the warmer Libyan waters. This eastward extension of the ATC (down to the Libyan shelf) corresponds to the Atlantic Libyan Current signature identified recently by *Gerin et al*. [2009] and *Sorgente et al*. [2011]. This Atlantic Libyan Current-like current on track 222 (blue squares line, Figure 10) appears from September to March. During the other seasons, the crossover AGVs of tracks 222-059 (Figure 11) show a current generally flowing southeastward from spring (5 cm/s) to fall (8 cm/s) toward the Libyan shelf. However, the opposite westward AGV on the southern end of track 222 suggests a deviation offshore of the eastward ATC outflow, possibly twisting over the Sidra Gyre northern arm. Indeed, the phasing of the averaged AGV on the Atlantic Libyan Current path and the southern part of the Sidra Gyre (red solid and blue squares line, Figure 10) confirms this finding. This joint seasonality and positions of the Atlantic Libyan Current and Sidra Gyre are consistent with recent works such as *Sorgente et al*. [2011], *Poulain and Zambianchi* [2007], and *Poulain et al*. [2012].

4.2.4. The Atlantic Ionian Stream

The southeastward AIS veins observed on the northern parts of tracks 237, 059, and 044 show a clear seasonal cycle, with maximum values in summer and fall (cyan, green and black solid lines, Figure 10) when the thermal front is well marked (Figure 11). This coherent phasing confirms a continuity of part of the Atlantic Water flow from the Tunisia-Sicily Channel entrance to the southern Sicily coast. As suggested by Figure 11, the AIS summer intensification is mainly due to the Sicily upwelling on Adventure Bank induced by the dominant summer and fall northwesterly winds [*Lermusiaux and Robinson*, 2001]. Close to Malta Island, the strong AIS southeast branch corresponding to the AIS (Figure 11, black and green solid lines on Figure 10) agrees with the findings of *Poulain and Zambianchi* [2007]. In winter, the AGV (off the Gulf of Hammamet on track 222 and on the northern part of track 059, Figure 11) meanders along the SST front from the Tunisian shelf to the Sicily coast, feeding the AIS. This is confirmed by analyzing the AGV time series of tracks passing over the Gulf of Hammamet (ATC continuation from Cape Bon) and the Malta Channel (AIS continuation toward the Italian coast). Indeed, the winter averaged AGVs at the Malta Channel (green solid line, Figure 10) represent 60% of the eastward flow going out of Hammamet (blue triangles line, Figure 10); the remaining part flows southward toward Lampedusa (green dashed line, Figure 10). Nevertheless, the AIS/ATC connection might play a minor part in the ATC flow in winter, producing the high intensity of the ATC related veins during this season. The eastern-most AIS branch on the crossover of tracks 044-135 (Figure 11) is accompanied by a thermal front separating the colder Ionian surface waters from the

warmer ones of the Gulf of Sirte. It shows a minimum in spring, consistent with the upward minimum on track 059 (black dashed and green solid lines, Figure 10).

4.3. Schematic View of the Regional Circulation

Based on the above analysis (Figures 9–11), we can now propose a new regional circulation scheme (Figure 12) for the seasonal surface circulation. Most of the feature names presented in Figure 12 are derived from *Lermusiaux and Robinson* [2001], *Béranger et al*. [2004], and *Sorgente et al*. [2011].

At the entrance of the Tunisia-Sicily Channel ($>\sim$36°N), the eastward Algerian Current shows a permanent bifurcation resulting in two branches: the upper Bifurcation Tyrrhenian Current flowing northward toward the Tyrrhenian basin and the lower ATC flowing southward into the Tunisia-Sicily Channel. The winter and spring patterns are quite similar. Following the SST front and AGV pattern/time series, the Atlantic Water flowing off the Gulf of Hammamet toward the Malta Channel feeds the AIS. Although its thermal signature is not obvious in spring, the AGV along tracks 222 and 059-044 support this result. The summer and fall situations also show similar patterns with some differences. Indeed, the Bifurcation Tyrrhenian Current splits west of Sicily in a southward branch, the AIS, strongly constrained by the Sicily upwelling. A particular summer pattern is that part of the weak ATC may join the AIS west of Cape Bon, whereas the other part continues southwestward to the Gulf of Hammamet. The fall season reveals two ways the AIS can be fed. The first is from the Gulf of Hammamet toward Malta Channel in winter, and the second is down from the Bifurcation Tyrrhenian Current bypassing the Adventure Bank Vortex in summer. Over all seasons, the AIS completes its journey to the Ionian Sea (heading North East) through the Malta Channel and toward the Gulf of Sirte (heading South East). We named this southeastern-most AIS outflow the Eastern Atlantic Ionian Stream.

Further south ($\sim$35°N–36°N), the circulation pattern is the same for all seasons. The ATC flows southeastward along the 200 m isobath from the Gulf of Hammamet to the central part of the Tunisia-Sicily Channel where it joins the Eastern Atlantic Ionian Stream. This western extension of the ATC was revealed by numerical modeling in *Sorgente et al*. [2011] as an unfamiliar feature called the Bifurcation Atlantic Tunisian Current. It was described as a stable and weak current flowing from November to April [*Sorgente et al*., 2011]. In this study, we observed the Bifurcation Atlantic Tunisian Current in both SST and AGV patterns all year long. Its pathway varies from one season to the other and is strongly related to the north-south thermal front of the Tunisia-Sicily Channel.

From the central part of the Tunisia-Sicily Channel to the Libyan coasts ($\sim<$35°N), the winter situation is characterized by the maximum southeastern extension of the ATC. Both the SST and the AGV patterns along track 059 suggest a vein that would first enter the Gulf of Gabes before again joining the 200 m isobath advecting the Atlantic Water southeastward toward the Libyan coast. The vein appears to feed the narrow Atlantic Libyan Current that flows southeastward during winter when the Sidra Gyre extension is most contracted compared with the rest of the climatological year. The other seasonal schemes are very similar. The main difference is the Sidra Gyre spatial expansion, which expands and intensifies in spring and summer and may then block the eastward ATC flow at the entrance of the Libyan shelf (approximately 33°N). The western arm of the Sidra Gyre likely helps to deviate the descending ATC flow to the North West (approximately 13°E). Over the Gulf of Gabes, the SST second front and the AGV pattern on track 059 suggest that part of the ATC would swirl to the North West, where it might then fuel the Bifurcation Atlantic Tunisian Current and the Eastern Atlantic Ionian Stream. Note that the Bifurcation Atlantic Tunisian Current position may also be linked to the Sidra Gyre eastern arm. This observation agrees with the findings of *Sorgente et al*. [2011] from numerical modeling. The Sidra Gyre would block the Atlantic Water advection along Libya, deviating the flow offshore (toward the open Ionian Sea).

5. Conclusion and Perspectives

The main purpose of this paper is to improve the description of the seasonal circulation variability of the central Mediterranean Sea by using 20 years (1993–2013) of along-track altimetry data over the areas surrounding the Tunisian coasts (Algerian/Tunisian, Tunisian and Tunisian/Libyan shelves). The study is based on recent releases of Level 3 altimetry products that include refined regional processing.

Cross comparisons of altimetry with in situ data and satellite Sea Surface Temperature images show that altimeter-derived geostrophic currents are able to capture the main surface circulation features. Despite the relatively good agreement between in situ and altimetry data, several questions still remain, such as the ability of tide gauges in harbors to measure the same sea level variations as those observed by altimetry further offshore. The comparison between ADCP currents and altimetry gestrophic velocities gives satisfying results without adding a wind-driven Ekman velocity component that may help to further reduce the root-mean-square difference [e.g., *Saraceno et al*., 2008; *Liu et al*., 2012].

The parallel use of standard regional (AVISO) and experimental (X-TRACK) altimeter products to estimate the geostrophic velocity provides robust assessments of conventional altimetry and offers the opportunity to analyze and quantify the impact of different data processing and corrections over the study area. Even if the results are globally consistent, the patterns derived from X-TRACK exhibit more space-time variations (Figures 3 and 8) and a better qualitative agreement with the satellite SST (Figure 7). The significant differences between both products especially appeared in qualitative comparisons with SST fields over the shallow water of the Gulf of Gabes (Figure 7). Moreover, the X-TRACK data set generally shows better agreements with in situ ADCP and tide gauge records and, more importantly, allows recovery of more suitable data (Figure 2). Hence, the X-TRACK product is considered more relevant than AVISO to monitor ocean features in coastal areas with wide continental shelves, such as the central Mediterranean Sea.

The analysis of satellite SST and 20 year altimetry-derived patterns (Figures 9–11) highlights a complex regional circulation with significant seasonal variations in the magnitudes and pathways of currents. In areas where the satellite tracks are almost perpendicular to the main flows, we observed the advection of Atlantic Waters from the Algerian to the Tunisian shelf and bifurcating into an upper Bifurcation Tyrrhenian Current branch and lower Atlantic Tunisian Current/Atlantic Ionian Stream veins. The Atlantic Tunisian Current (Atlantic Ionian Stream) is stronger (weaker) in winter and less (more) marked in summer. These periods of maxima and minima correspond to those reported by *Ciappa* [2009], *Sorgente et al*. [2003, 2011], and *Hamad et al*. [2006]. The continuation of these features from the Tunisian/Sicilian to the Libyan shelves revealed a marked Atlantic Libyan Current flowing along the 200 m isobath in winter, when the Sidra Gyre extension is reduced. Over all seasons, we observed the Bifurcation Atlantic Tunisian Current flowing near the western arm of Sidra Gyre toward the Ionian Sea, where it joins the Eastern Atlantic Ionian Stream. These space/time characterizations obtained from altimetry allow us to propose a new schematic circulation pattern (Figure 12) for the different seasons. This new scheme is consistent with the recent works of *Ciappa* [2009] and *Sorgente et al*. [2011] by extending their results over a larger spatial and temporal coverage. The persistence of the observed circulation features at a climatological scale indicates their recurrent character, especially the connection of the Atlantic Tunisian Current with the Atlantic Libyan Current in winter. Moreover, this study confirms the suspected branches of the southern-most Atlantic Tunisian Current bifurcations: the Bifurcation Atlantic Tunisian Current observed by *Gerin et al*. [2009] and *Ciappa* [2009] and the western branches from the Libyan shelf/the exit of the Gulf of Hammamet toward the Gulf of Gabes, modeled by *Sorgente et al*. [2011] and here observed for the first time.

This paper shows the ability of conventional altimetry to characterize the circulation seasonal variability in the study area. However, the long-term continuity of the TP+J1+J2 time series would be relevant to provide first insights on the inter-annual component. Further work is needed to fully understand the differences between year-to-year fluctuations, the trend changes and the forcing mechanisms. This is clearly beyond the scope of the present study and will be the subject of a future paper.

As a next step, there is no doubt that the synergistic use of altimetry with regional modeling and complementary observing systems (in situ data, HF radars, surface drifters, satellite remote sensing data) should allow resolution of a wider spectrum of spatial and temporal scales of variability [*Birol et al*., 2010]. Despite coastal-oriented altimetry postprocessing approaches, the study of the relatively narrow slope currents from pulse-limited conventional altimetry remains challenging because of instrumental issues and the inaccuracy of some geophysical corrections. However, this study demonstrates that, when carefully analyzed, the derived geostrophic currents can be exploited to detect the regional circulation in the central Mediterranean.

The use of long-term conventional pulse-limited altimetry data to study coastal ocean circulation and variability is therefore highly promising, especially in regions where the circulation is poorly sampled and

documented. The new generation of altimetry missions, such as the ESA Earth Explorer Mission Cryosat-2 (SAR/SARIN mode), the CNES/ISRO SARAL-AltiKa Mission (Ka-band) as well as the COPERNICUS Sentinel-3, Sentinel-6 Mission (SAR mode), will offer very promising perspectives over the coastal domains by significantly reducing measurement noise and increasing the along-track resolution. Future complementary swath altimetry data from the NASA/CNES SWOT mission (Ka-band Radar Interferometer) should provide a higher 2-D horizontal resolution (i.e., 1 km) in addition to across-track measurements that hold the promise of improved monitoring capabilities over the coastal domain.

Acknowledgments

This work is part of the PhD of Madame Jebri Fatma. This publication was produced with the financial support of the Allocations de recherche pour une thèse au sud (ARTS) program of the Institut de recherche pour le développement (IRD). The standard altimeter products were produced and distributed by AVISO (http://www.aviso.altimetry.fr/en/data/products/sea-surface-height-products/regional/) as part of the SSALTO ground-processing segment. The X-TRACK altimetry data used in this study were developed, validated, and distributed by the CTOH/LEGOS, France (http://ctoh.legos.obs-mip.fr/products/coastal-products/coastal-products-1/sla-1hz/medsea/). The authors kindly acknowledge the PSMSL (http://www.psmsl.org/data/obtaining/) and IHE (rafik-ihe@planet.tn) networks for the tide gauge sea level records. The authors would also like to thank Katrin Schroeder (CNR-ISMAR), Gian Pietro Gasparini (CNR-ISMAR), and Sana Ben Ismail (INSTM) for the processed and validated ADCP current data (katrin.shroeder@ismar.cnr.it). The authors wish to thank the MyOcean project (http://marine.copernicus.eu/web/69-interactive-catalogue.php?option=com_csw&view=details&product_id=SST_MED_SST_L3S_NRT_OBSERVATIONS_010_012) for providing daily SST images. We wish to acknowledge the contribution of the center that provides the weekly SST images: the DLR (German Space Center (http://www.dlr.de/eoc/en/desktopdefault.aspx/tabid-8799/).

References

Alhammoud, B., K. Béranger, L. Mortier, M. Crépon, and I. Dekeyser (2004), Surface circulation of the Levantine basin: Comparison of model results with observations, *Prog. Oceanogr.*, *66*(2-4), 299–320.

Ben Ismail, S., C. Sammari, G. P. Gasparini, K. Béranger, M. Brahim, and L. Aleya (2012), Water masses exchanged through the Sicily Channel: Evidence for the presence of new water masses on Tunisian side of the Channel, *Deep Sea Res.*, Part I, *63*(2012), 65–81.

Béranger, K., L. Mortier, G. P. Gasparini, L. Gervasio, M. Astraldi, and M. Crepon (2004), The dynamics of the Sicily strait: A comprehensive study from observations and models, *Deep Sea Res., Part II*, *51*, 411–440.

Birol, F., M. Cancet, and C. Estournel (2010), Aspects of the seasonal variability of the Northern Current (NW Mediterranean Sea) observed by altimetry, *J. Mar. Syst.*, *81*, 297–311.

Bouffard, J., S. Vignudelli, P. Cipollini, and Y. Menard (2008), Exploiting the potential of an improved multimission altimetric data set over the coastal ocean, *Geophys. Res. Lett.*, *35*, L10601, doi:10.1029/2008GL033488.

Bouffard, J., A. Pascual, S. Ruiz, Y. Faugère, and J. Tintoré (2010), Coastal and mesoscale dynamics characterization using altimetry and gliders: A case study in the Balearic, Sea, *J. Geophys. Res.*, *115*, C10029, doi:10.1029/2009JC006087.

Bouffard, J., L. Roblou, F. Birol, A. Pascual, L. Feneglio-Marc, M. Cancet, R. Morrow, and Y. Menard (2011), Introduction and assessment of improved coastal altimetry strategies: Case study over the North Western Mediterranean Sea, in *Coastal Altimetry*, edited by S. Vignudelli et al., Springer, Berlin.

Buongiorno Nardelli, B., C. Tonconi, A. Pisano, and R. Santoleri (2013), High and Ultra-High resolution processing of satellite Sea Surface Temperature data over Southern European Seas in the framework of MyOcean project, *Remote Sens. Environ*, *129*, 1–16.

Carrère, L., and F. Lyard (2003), Modeling the barotropic response of the global ocean to atmospheric wind and pressure forcing—Comparisons with observations, *Geophys. Res. Lett.*, *30*(6), 1275, doi:10.1029/2002GL016473.

Ciappa, A. C. (2009), Surface circulation patterns in the Sicily Channel and Ionian Sea as revealed by MODIS chlorophyll images from 2003 to 2007, *Cont. Shelf Res.*, *29*, 2099–2109.

CNR IAMC and CNR ISMAR (2009), *Cruise Report–SICILY09*, edited by A. Ribotti and M. Borghini.

Deng, X., C. Hwang, R. Coleman, and W. E. Featherstone (2008), Seasonal and interannual variations of the Leeuwin Current off Western Australia from TOPEX/Poseidon Satellite Altimetry, *Terr. Atmos. Ocean Sci.*, *19*(1–2), 135–149.

Dufau, C., S. Labroue, G. Dibarboure, Y. Faugère, I. Pujol, C. Renaudie, and N. Picot (2013), Reducing altimetry small-scale errors to access (sub)mesoscale dynamics, Ocean Surface Topography Science Team Meeting, 811 October. [Available at http://www.aviso.altimetry.fr/fileadmin/documents/OSTST/2013/oral/Dufau_PresentationError_FINAL.pdf.]

Durand, F., D. Shankar, F. Birol, and S. S. C. Shenoi (2008), Estimating boundary currents from satellite altimetry: A case study for the east coast of India, *J. Oceanogr.*, *64*, 831–845, doi:10.1007/s10872-008-0069-2.

Fu, L. L., and R. Morrow (2013), Remote sensing of the global ocean circulation,ocean circulation and climate—A 21st century perspective, *Int. Geophys.*, *103*, 83–111.

Fu, L. L., and R. D. Smith (1996), Global ocean circulation from satellite altimetry and high-resolution computer simulation, *Bull. Am. Meteorol. Soc.*, *77*, 2625–2636.

Gasparini, G.P., K. Schroder, A. Vetrano and M. Astraldi (2007), Canali e stretti quali punti di osservazione privilegiata per lo studio della variabilita interannuale del bacino Mediterraneo, In: Clima e cambiamenti climatici: le attivita di ricerca del CNR. CNR Roma (Ed.), pp. 521–524.

Gasparini, G. P., A. Bonanno, S. Zgozi, G. Basilone, M. Borghini, G. Buscaino, A. Cuttitta, N. Essarbout, S. Mazzola, B. Patti, A.B. Ramadan, K. Schroeder, T. Bahri and F. Massa (2008), Evidence of a dense water vein along the Libyan continental margin, *Ann. Geophys.*, *26*, 1–6, doi:10.5194/angeo-26-1-2008.

Gerin, R., P.-M. Poulain, I. Taupier-Letage, C. Millot, S. Ben Ismail, and C. Sammari (2009), Surface circulation in the Eastern Mediterranean using drifters (20052007), *Ocean Sci.*, *5*, 559–574, doi:10.5194/os-5-559-2009.

Hamad, N., C. Millot, and I. Taupier-Letage (2006), The surface circulation in the eastern basin of the Mediterranean, Sea. *Sci. Mar.*,*70*, 457–503.

Holgate, S. J., et al. (2013), New data systems and products at the permanent service for mean sea level, *J. Coastal Res.*, *29*(3), 493–504.

Le Hénaff, M., L. Roblou, and J. Bouffard (2011), Characterizing the Navidad Current interannual variability using coastal altimetry, *Ocean Dyn.*, *61*(4), 425–437.

Lermusiaux, P. F. J., and A. R. Robinson (2001), Features of dominant mesoscale variability, circulation patterns and dynamics in the Strait of Sicily, *Deep Sea Res., Part I*, *48*, 1953–1997.

Le Traon, P. Y., and F. Ogor (1998), ERS-1/2 orbit improvement using TOPEX/POSEIDON: The 2 cm challenge, *J. Geophys. Res.*, *103*, 8045–8057.

Liu, Y., R. H. Weisberg, S. Vignudelli, L. Roblou, and C. R. Merz (2012), Comparison of the X-TRACK altimetry estimated currents with moored ADCP and HF radar observations on the West Florida Shelf, J. *Adv. Space Res.*, *50*(8), 1085–1098.

Millot, C. (1999), Circulation in the Western Mediterranean Sea, *J. Mar. Syst.*, *20*, 423–442.

Molcard, A., L. Gervasio, A. Griffa, G. P. Gasparini, L. Mortier, and T. M. Ozgokmen (2002), Numerical investigation of the Sicily Channel dynamics: Density current and water mass advection, *J. Mar. Syst.*, *36*, 219–238.

Morrow, R., R. Coleman, J. Church, and D. Chelton (1994), Surface eddy momentumflux and velocity variances in the southern ocean from Geosat altimetry, *J. Phys. Oceanogr.*, *24*, 2050–2071.

Parke, M. E., R. L. Stewart, D. L. Farless, and D. E. Cartwritght (1987), On choice of orbits for an altimetric satellite to study ocean circulation and tides, *J. Geophys. Res.*, *92*, 11,693–11,707.

Pawlowicz, R., B. Beardsley, and S. Lentz (2002), Classical tidal harmonic analysis with errors in matlab using t-tide, *Comput. Geosci.*, *28*, 929–937.

Poulain, P. M., and E. Zambianchi (2007), Surface circulation in the central Mediterranean Sea as deduced from Lagrangian drifters in the 1990s, *Cont. Shelf Res.*, *27*(7), 981–1001.

Poulain, P. M., M. Menna, and E. Mauri (2012), Surface geostrophic circulation of the Mediterranean Sea derived from drifter and satellite altimeter data, *J. Phys. Oceanogr.*, *42*, 973–990.

Powell, B. S., and R. P. Leben (2004), An optimal filter for geostrophic mesoscale currents from along-track satellite altimetry, *J. Atmos. Oceanic Technol.*, *21*, 1633–1642.

Powell, B. S., R. R. Leben, and N. L. Guinasso (2006), Comparison of Buoy and altimeter-derived Shelf currents using an optimal operator, *IEEE Geosci. Remote Sens. Lett.*, *3*, 192–196.

Rio, M.-H., A. Pascual, P.-M. Poulain, M. Menna, B. Barceló, and J. Tintoré (2014), Computation of a new Mean Dynamic Topography for the Mediterranean Sea from model outputs, altimeter measurements and oceanographic *in situ* data, *Ocean Sci. Discuss.*, *11*, 655–692.

Robinson, A. R., J. Sellshop, A. Warn-Varnas, W. G. Leslie, C. J. Lozano, P. J. Haley Jr., L. A. Anderson, and P. J. F. Lermusiaux (1999), The Atlantic Ionian stream, *J. Mar. Syst.*, *20*, 129–156.

Roblou, L., J. Lamouroux, J. Bouffard, F. Lyard, M. Le Hénaff, A. Lombard, P. Marsalaix, P. De Mey, and F. Birol (2011), Post-processing altimeter data toward coastal applications and integration into coastal models, in *Coastal Altimetry*, chap. 9, edited by S. Vignudelli et al., Springer, Berlin.

Sammari, C., C. Millot, I. Taupier Letage, A. Stefani, and M. Brahim (1999), Hydrological characteristics in the Tunisia–Sardinia–Sicily area during spring 1995, *Deep Sea Res.*, Part I, *46*, 1671–1703.

Saraceno, M., P. T. Strub, and P. M. Kosro (2008), Estimates of sea surface height and near surface alongshore coastal currents from combinations of altimeters and tide gauges, *J. Geophys. Res.*, *113*, C11013, doi:10.1029/2008JC004756.

Sorgente, R., A. F. Drago, and A. Ribotti (2003), Seasonal variability in the Central Mediterranean Sea circulation, *Ann. Geophys.*, *21*, 299–322, doi:10.5194/angeo-21-299-2003.

Sorgente, R., A. Olita, P. Oddo, L. Fazioli, and A. Ribotti (2011), Numerical simulation and decomposition of kinetic energies in the Central Mediterranean Sea: Insight on mesoscale circulation and energy conversion, *Ocean Sci. Discuss.*, *8*, 1-54.

Strub, P. T., T. K. Chereskin, P. P. Niiler, C. James, and M. D. Levine (1997), Altimeter derived variability of surface velocities in the California current system: 1. Evaluation of TOPEX/POSEIDON altimeter velocity resolution, *J. Geophys. Res.*, *102*, 12,727–12,748.

Taupier-Letage, I. (2008), On the use of thermal images for circulation studies: Applications to the Eastern Mediterranean basin, in *Remote Sensing of the European Seas*, pp. 153–164, Part 2, Springer, Netherlands.

Taylor, K. E. (2001), Summarizing multiple aspects of model performance in a single diagram, *J. Geophys. Res.*, *106*, 7183–7192.

Vignudelli, S., P. Cipollini, L. Roblou, F. Lyard, G. P. Gasparini, G. Manzella, and M. Astraldi (2005), Improved satellite altimetry in coastal systems: Case study of the Corsica Channel (Mediterranean Sea), *Geophys. Res. Lett.*, *32*, L07608, doi:10.1029/2005GL022602.